AGU PUBLICATIONS

Earth's Future

RESEARCH ARTICLE
10.1002/2017EF000620

Quantifying and Comparing Effects of Climate Engineering Methods on the Earth System

Sebastian Sonntag[1], Miriam Ferrer González[1,2], Tatiana Ilyina[1], Daniela Kracher[1], Julia E. M. S. Nabel[1], Ulrike Niemeier[1], Julia Pongratz[1], Christian H. Reick[1], and Hauke Schmidt[1]

[1]Max Planck Institute for Meteorology, Hamburg, Germany, [2]International Max Planck Research School on Earth System Modelling, Hamburg, Germany

Key Points:
- More carbon needs to be taken up on land under reforestation than by ocean under alkalinization to reach the same global warming reduction
- Solar radiation management causes enhanced land carbon uptake and reduced atmospheric CO_2
- Choice of variables and normalization of results are essential for a quantitative comparison of climate engineering methods

Correspondence to:
S. Sonntag,
sebastian.sonntag@mpimet.mpg.de

Citation:
Sonntag, S., González, M. F., Ilyina, T., Kracher, D., Nabel, J. E. M. S., Niemeier, U., Pongratz, J., Reick, C. H., & Schmidt, H. (2018). Quantifying and Comparing Effects of Climate Engineering Methods on the Earth System, *Earth's Future*, *6*, 149–168, https://doi.org/10.1002/2017EF000620

Received 5 DEC 2017
Accepted 15 JAN 2018
Accepted article online 24 JAN 2018
Published online 5 FEB 2018

Abstract To contribute to a quantitative comparison of climate engineering (CE) methods, we assess atmosphere-, ocean-, and land-based CE measures with respect to Earth system effects consistently within one comprehensive model. We use the Max Planck Institute Earth System Model (MPI-ESM) with prognostic carbon cycle to compare solar radiation management (SRM) by stratospheric sulfur injection and two carbon dioxide removal methods: afforestation and ocean alkalinization. The CE model experiments are designed to offset the effect of fossil-fuel burning on global mean surface air temperature under the RCP8.5 scenario to follow or get closer to the RCP4.5 scenario. Our results show the importance of feedbacks in the CE effects. For example, as a response to SRM the land carbon uptake is enhanced by 92 Gt by the year 2100 compared to the reference RCP8.5 scenario due to reduced soil respiration thus reducing atmospheric CO_2. Furthermore, we show that normalizations allow for a better comparability of different CE methods. For example, we find that due to compensating processes such as biogeophysical effects of afforestation more carbon needs to be removed from the atmosphere by afforestation than by alkalinization to reach the same global warming reduction. Overall, we illustrate how different CE methods affect the components of the Earth system; we identify challenges arising in a CE comparison, and thereby contribute to developing a framework for a comparative assessment of CE.

1. Introduction

Several measures to deliberately manipulate the global climate and thereby reduce the risks of substantial anthropogenic climate change have been proposed (e.g., Caldeira et al., 2013). These climate engineering (CE; or geoengineering) methods aim at reducing either the amount of solar radiation reaching the surface of the Earth (solar radiation management, SRM) or the atmospheric CO_2 concentration (carbon dioxide removal, CDR). While a full understanding of the potential consequences of CE methods is still missing, the role of CDR (or "negative emissions") and of SRM in climate policy is increasingly discussed, in particular in the context of the Paris Agreement (Fuss et al., 2016; Hansen et al., 2017; Horton et al., 2016; Parson, 2017; Sanderson et al., 2016; United Nations Framework Convention on Climate Change [UNFCCC], 2015; Williamson, 2016).

Modeling projects, such as the Geoengineering Model Intercomparison Project (GeoMIP; Kravitz et al., 2013b) have contributed to our understanding of CE. However, GeoMIP so far is limited to SRM and complementary approaches to study CDR such as CDR-MIP (Keller et al., 2017) have been initiated only recently. Other modeling projects have contributed to the understanding of the global carbon cycle (C4MIP; Friedlingstein et al., 2006; Arora et al., 2013) and land-use changes (LUCID; Brovkin et al., 2013), but were not specifically designed to study CE and were not used to assess land- and ocean-based CE measures.

Being different concepts, CDR and SRM have been assessed separately in earlier reports (National Research Council [NRC], 2015a, 2015b). Yet, other reports have assessed CDR and SRM methods comparatively (Rickels et al., 2011; Royal Society, 2009; Schäfer et al., 2015; Vaughan & Lenton, 2011) and state the usefulness of a common assessment framework for all response options—CE methods, mitigation, and adaptation (Intergovernmental Panel on Climate Change [IPCC], 2012). In addition, several authors (e.g., Klepper &

Rickels, 2012; Victor, 2008) have emphasized that the response to climate change will likely be a portfolio of mitigation, adaptation, and a subportfolio of CE measures. To arrive at such a portfolio, the comparison of these very different measures is a prerequisite. Also, the need for integrated research on CE has been emphasized (Oschlies & Klepper, 2017), in particular on the carbon effects of SRM (Keith et al., 2017). The IPCC's Fifth Assessment Report summarizes that, although some robust responses to some SRM methods have been found, there is insufficient knowledge concerning CDR and a "comprehensive quantitative assessment" of CE in general is not possible (IPCC, 2013). Furthermore, for example afforestation is an already implemented part of policy measures based on CE (UNFCCC, 2012). Thus, to go beyond understanding individual CE methods and to investigate how a CE comparison can be performed in a quantitative way is crucially needed at this point in time where CE is discussed as policy implementation. We refrain from suggesting that quantitative results of modeling studies themselves should be used for this purpose, but the challenges and possible solutions for a quantitative comparison provide the basis for closing the gap identified by the IPCC.

Previous reports were mostly based on studies of individual CE methods, which makes it difficult to assess different CE methods in a comparative way. Previous SRM model studies have focused mainly on comparing the same SRM method simulated by different models (e.g., Kravitz et al., 2013a) or on comparing various SRM methods simulated within one model (e.g., Niemeier et al., 2013). Concerning CDR, model studies have used different scenarios and also different types of models (e.g., Boucher et al., 2012; Cao & Caldeira, 2010; Gasser et al., 2015; Jones et al., 2016; Zickfeld et al., 2013). A comparison of a range of different CE methods within one model framework, however, so far has only been performed by Keller et al. (2014) using an Earth system model of intermediate complexity.

Using a state-of-the-art, comprehensive Earth system model to assess key CE methods, this study goes beyond previous qualitative assessments (e.g., Royal Society, 2009) and comparative approaches that drew from different individual studies. Furthermore, we compare the intended effects of the CE methods and of mitigation efforts to possible unintended effects and feedbacks (e.g., Vaughan & Lenton, 2011). We use the Max Planck Institute Earth System Model (MPI-ESM) that includes general circulation models for atmosphere and ocean and models for the land surface, the terrestrial biosphere, and marine biogeochemistry. We use MPI-ESM with an interactive carbon cycle and prognostic atmospheric CO_2 concentrations. We compare SRM by stratospheric sulfur injection with two CDR methods: afforestation and ocean alkalinization. We perform model experiments each including one of the three CE methods and all forced by fossil-fuel CO_2 emissions according to the high-emission scenario RCP8.5 (Riahi et al., 2011) that assumes no mitigation policy.

This study aims at quantifying the effects of different CE methods on different components of the Earth system, at illustrating different targets and effects, and at contributing to a better understanding of how interactions and feedbacks between Earth system components lead to certain responses. As we are studying the effects of different anthropogenic interferences on the Earth system from a natural science perspective and not the response to these changes without affecting them, we do not include adaptation in our study. We identify and illustrate challenges and the intrinsic complexity that arises in a comparative assessment of CE. Rather than investigating technical or economic feasibility of the CE methods, which may in the end be additional important factors to account for in an assessment of CE and are discussed, for example, by Klepper and Rickels (2014), NRC (2015a, 2015b), Harding and Moreno-Cruz (2016), Moriyama et al. (2017), and Niemeier and Tilmes (2017), we focus on studying the simulated Earth system response to a potential deployment of the methods.

2. Methods

2.1. Model Configuration and Experiments

For all model experiments (see overview in Table 1) we use the MPI-ESM in the low resolution (LR) configuration with a T63 (1.9°) horizontal resolution and 47 hybrid sigma-pressure levels for the atmosphere and a bipolar grid with 1.5° resolution (near the equator) and 40 unevenly spaced vertical levels for the ocean (Giorgetta et al., 2013). The MPI-ESM includes the general circulation models for atmosphere ECHAM6 (Stevens et al., 2013) and ocean MPIOM (Jungclaus et al., 2013), the model JSBACH for the land surface and the terrestrial biosphere including dynamic vegetation (Reick et al., 2013), and the model HAMOCC5 for marine biogeochemistry (Ilyina et al., 2013a, 2013b). MPI-ESM includes a fully coupled carbon-cycle model

Table 1.
Overview of the Model Experiments Used in This Study

Experiment name	CO_2 forcing	Land-use transitions	Other forcings
rcp85	RCP8.5 fossil-fuel emissions	RCP8.5	RCP8.5
CE-atmos	RCP8.5 fossil-fuel emissions	RCP8.5	RCP8.5 + stratospheric aerosol enhancement
CE-ocean	RCP8.5 fossil-fuel emissions	RCP8.5	RCP8.5 + ocean alkalinity enhancement
CE-land	RCP8.5 fossil-fuel emissions	RCP4.5	RCP8.5
rcp45	RCP4.5 concentrations	RCP4.5	RCP4.5
hist	Historical fossil-fuel emissions	Historical	Historical

Note. Detailed descriptions are given in Section 2.

with interactive atmospheric CO_2. This means that atmosphere, land, and ocean can exchange carbon in response to given fossil-fuel CO_2 emissions, while the resulting atmospheric CO_2 concentration and the various land and ocean carbon pools are calculated prognostically.

We use the same model configuration as for the Coupled Model Intercomparison Project Phase 5 (CMIP5) experiment *esmrcp85* (Reick et al., 2012a), which serves as a reference experiment and which we refer to as "rcp85" here. In addition to this emission-driven model experiment, for comparison we also use the CMIP5 experiment *rcp45* (called "rcp45" here, Giorgetta et al. (2012)), which is driven by CO_2 concentrations according to RCP4.5 (Thomson et al., 2011).

All CE model experiments are driven by CO_2 emissions due to fossil-fuel burning and cement production, while atmospheric CO_2 concentrations are calculated prognostically. All experiments also use the same boundary data for Earth orbit parameters and solar irradiance, as well as for atmospheric concentrations of CH_4, N_2O, CFCs, ozone, and aerosols according to RCP8.5. The SRM model experiment uses an additional aerosol forcing as described below. In all experiments, we use the land-use harmonization dataset according to Hurtt et al. (2011), which provides transitions between different land-use types and information on wood harvest based on global gridded land-use change scenarios. In MPI-ESM, the transitions between crops, pasture, and natural vegetation types as well as the distribution of natural vegetation among different plant functional types are simulated as described by Reick et al. (2013). Since the model includes an interactive carbon cycle, CO_2 emissions due to land-use changes are calculated prognostically according to the given land-use transitions. All experiments are initialized from the end of the historical CMIP5 experiment *esmHistorical* (called "hist" here, Reick et al. (2012b)) at the beginning of the year 2006 and are run until the year 2100.

Not all processes and components that may play a role in adequately representing the response of the Earth system to the simulated forcings are included in our model. For example, the model does not include permafrost, which would lead to an additional warming in warmer (e.g., RCP8.5) compared to colder (e.g., RCP4.5) scenarios (e.g., Schaefer et al., 2014) and thus could lead to an underestimation of the cooling effects of the CE methods. Our model also lacks a nitrogen cycle, which could affect the carbon response in the reference and in the CE experiments (e.g., Kracher, 2017). However, potentially overestimated terrestrial productivity and carbon content partly cancel out when looking at differences between model experiments. Also, a high increase of gross primary productivity historically, as simulated by MPI-ESM, is in line with newest evidence (Campbell et al., 2017) and for soil carbon most models show an increase for most scenarios (Jones et al., 2013). Altogether, the published simulations are within the range of those of other CMIP5 models, thus our results should be representative of current state-of-the-art.

2.2. CE Model Experiments

The three CE model experiments describe scenarios in which the effect of fossil-fuel burning on global mean surface air temperature under the RCP8.5 scenario is offset to follow, or at least get closer to, the RCP4.5 scenario. They are SRM via stratospheric sulfur injection, CDR via ocean alkalinization, and CDR via afforestation. We compare the CE methods, which are frequently discussed but very different in their approach, to each

other and to the reference scenarios RCP8.5 and RCP4.5. We choose RCP4.5 as target scenario because it constitutes a substantial climate difference to RCP8.5 and provides a scenario of mitigation options to compare CE to. Since SRM targets radiation, the deployment of this CE is chosen such that the net radiative forcing follows the RCP4.5 trajectory. As CDR targets CO_2, for the ocean alkalinization scenario the deployment is such that the atmospheric CO_2 concentration in the CE model experiment follows the RCP4.5 trajectory. For CDR via afforestation we follow a different approach by choosing a well-defined land-use scenario, namely the one according to RCP4.5, leading to a substantial global increase of forest. As stated before, we do not aim at studying technical feasibility here, but in contrast to atmosphere- and ocean-based CE methods, very strong afforestation will directly collide with also other concerns because of the trade-offs with food security (e.g., Erb et al., 2016; Foley et al., 2011) and other ecosystem services (e.g., McCormack et al., 2016). Furthermore, extreme land-use change scenarios will have very much scenario-dependent features such as desert irrigation and its specific biogeophysical effects (Keller et al., 2014; Kemena et al., 2017). For these reasons, we stay with a scenario that has been identified as being a plausible future land-use change and that is part of the same RCP framework that our study is embedded in. Since this afforestation experiment is expected to show substantially smaller climate effects than the other two CE experiments, in our analysis we suggest ways to allow for a comparison despite such differences in the experimental setup. In all experiments the CE deployment starts in the year 2006 and is continued until the year 2100. In the following we describe the experimental setups in more detail.

The SRM model experiment, called "CE-atmos," describes enhancement of stratospheric aerosols by sulfur injection and is similar to the GeoMIP experiment G6sulfur (Kravitz et al., 2015). The injection in the model is done such that the net anthropogenic radiative forcing in RCP8.5 is counterbalanced to follow the radiative forcing trajectory as in RCP4.5. Since aerosol concentrations are not calculated explicitly in the model, the effects of the aerosols on radiation are prescribed in terms of their optical properties. We follow the approach by Niemeier et al. (2013) and derive these properties from simulations with the aerosol microphysical model HAM (Stier et al., 2005) coupled to the general circulation model MAECHAM5 (Giorgetta et al., 2006). In those simulations, SO_2 is injected into one grid box at the equator. Transport causes a zonally relatively homogeneous and meridionally symmetric aerosol distribution with maxima around the equator and in the mid latitudes. Details are described in Niemeier and Timmreck (2015).

The ocean-based CE model experiment, called "CE-ocean," is described in Ferrer González and Ilyina (2016) and simulates enhancement of ocean alkalinity using calcium compounds. In this model experiment, total alkalinity is increased globally uniformly in the uppermost ocean model level (i.e., in the upper 12 m of the ocean) such that the atmospheric CO_2 concentration follows the RCP4.5 trajectory: technically, this is achieved by adding alkalinity when during the simulation the difference in atmospheric CO_2 to the one in RCP4.5 is larger than 1%. This spatially homogeneous global application of alkalinization is not a realistic scenario, but it allows studying the potential effects of this method in an idealized way.

The land-based CE model experiment, called "CE-land," is described in Sonntag et al. (2016) and simulates large-scale regrowth of forest on abandoned agricultural land. As a CDR method, increase in forest area aims at enhancing the natural terrestrial carbon sequestration. The experimental setup differs from the reference experiment rcp85 only in the land-use transitions and wood harvest rates: they are taken from RCP4.5 in experiment CE-land, describing large-scale abandonment of agricultural land and subsequent reforestation. In contrast, in experiments rcp85, CE-atmos, and CE-ocean the land-use transitions are taken from RCP8.5, which includes deforestation in large parts of the world.

2.3. Choice of Variables for Analysis

It is an open question which aspects of climate should be included in a comparative assessment of CE methods (Oschlies et al., 2016). Naturally, the focus is on surface air temperature, because the main aim of CE is to combat global warming and because changes in regional climate variables that local stakeholders and decision-makers can relate to are correlated with changes in global mean surface air temperature (Seneviratne et al., 2016). But since these correlations may no longer hold when introducing additional forcings by CE, as a proxy for water availability in terrestrial ecosystems, also changes in precipitation are taken into account. In addition, the different CE methods tackle their main target temperature reduction by means of different processes. SRM targets the short-wave radiative forcing and reduces the incoming solar radiation, whereas CDR methods target the land or ocean carbon sinks and reduce absorption of long-wave radiation

by CO_2 in the atmosphere. Therefore, certain process-specific variables will be affected more intensely than others and thus must be included in a comparative assessment. Examples are changes in radiative fluxes for SRM and carbon cycle aspects for CDR methods. Accordingly, the set of variables entering a comparative assessment is not independent of the CE measures considered, which makes general statements about preferential CE methods problematic.

In the present study we focus our analysis on the variables surface air temperature and precipitation as being most relevant for the characterization of climate conditions for living, on variables specific to the measures considered, and on variables that help understand the underlying processes: Net radiation at the top of the atmosphere as suggested by SRM, atmospheric CO_2 as main target variable of the CDR methods, net primary productivity (NPP) for land and ocean as important quantities characterizing the biological processes modified by them, and the carbon stocks as main drivers of temperature changes and for disentangling the carbon-driven changes from those driven by other forcings, such as aerosols or biogeophysical effects. While focusing our analysis on global annual mean changes induced by the CE methods, we also analyze the CE effects on spatial patterns and extremes of surface air temperature. Since we aim at providing a wide overview of Earth system effects of the CE methods, we limit our analysis in some aspects such as the hydrological effects. Nevertheless, we also partly analyze the CE effects on precipitation minus evaporation. While we do not explicitly distinguish between effects and side effects in this study, we would like to stress that some CE effects may be intended and others may not and that this distinction may be different for different CE methods. Effects of SRM have been studied, for example, by Pongratz et al. (2012) on agriculture and by Pitari et al. (2014) on stratospheric ozone, and Davies-Barnard et al. (2015) study sea ice effects of afforestation. Climate impacts of SRM have been reviewed by Irvine et al. (2017). Impacts of SRM and CDR methods on ecosystems are assessed by Russell et al. (2012) and McCormack et al. (2016).

3. Results and Discussion

3.1. Climate and Carbon Cycle Effects of CE Methods

The three different simulated CE methods have different effects on the climate and on the carbon cycle. In the following we give an overview of these effects as simulated in the three CE model experiments compared to the reference experiment rcp85 and partly also in comparison to experiment rcp45. Complementary analyses are given in Ferrer González and Ilyina (2016) for the ocean alkalinization experiment CE-ocean and in Sonntag et al. (2016) for the reforestation experiment CE-land.

3.1.1. Stratospheric Sulfur Injection

The idea of injecting sulfur particles into the stratosphere and thereby increasing the fraction of incoming solar radiation that is reflected back to space is one of the earliest proposed CE measures and has been one of the most discussed SRM methods (Budyko, 1977; Crutzen, 2006; Irvine et al., 2016; Niemeier & Tilmes, 2017). In our model experiment CE-atmos, the sulfur injections increase over the course of the century and reach almost 20 Mt S yr^{-1} by the year 2100 (Figure 1a), corresponding to a forcing about 2–3 times higher than that of the 1991 Mount Pinatubo eruption (Niemeier & Timmreck, 2015). The net radiation at the top of the atmosphere, resulting from the radiative forcing and the feedbacks within the Earth system, is similar to the one in experiment rcp45 (Figure 2a). The altered radiative forcing in CE-atmos leads to a surface air temperature that is close to but slightly higher than the one in rcp45 (Figure 2b), especially in the Arctic due to the disproportionally lower aerosol forcing in the high latitudes compared to the topics and mid latitudes. This higher global mean temperature is due to an imperfect compensation of the forcings. SRM leads to a global mean cooling of 1.83 K averaged over the years 2081–2100 compared to experiment rcp85, with more pronounced cooling in the Arctic and more pronounced cooling over land than over ocean (Figure 3a). For an overview of changes in key Earth system variables in the different model experiments see also Table 2.

Previous studies have analyzed the effect of SRM on extremes in idealized model simulations and indicate that temperature extremes may be affected differently than annual means (Aswathy et al., 2015; Curry et al., 2014). We find that the difference in the multiannual mean surface air temperature of the warmest day of a year between CE-atmos and rcp85 is more pronounced over land compared to sea than the annual mean (Figure 3b), whereas the Arctic amplification of the signal is stronger for the annual mean difference (Figure 3a). This indicates that the simulated spatial pattern of the cooling effect of SRM is different for the annual mean than for the warm extreme. The spatial pattern of the difference in the multiannual mean

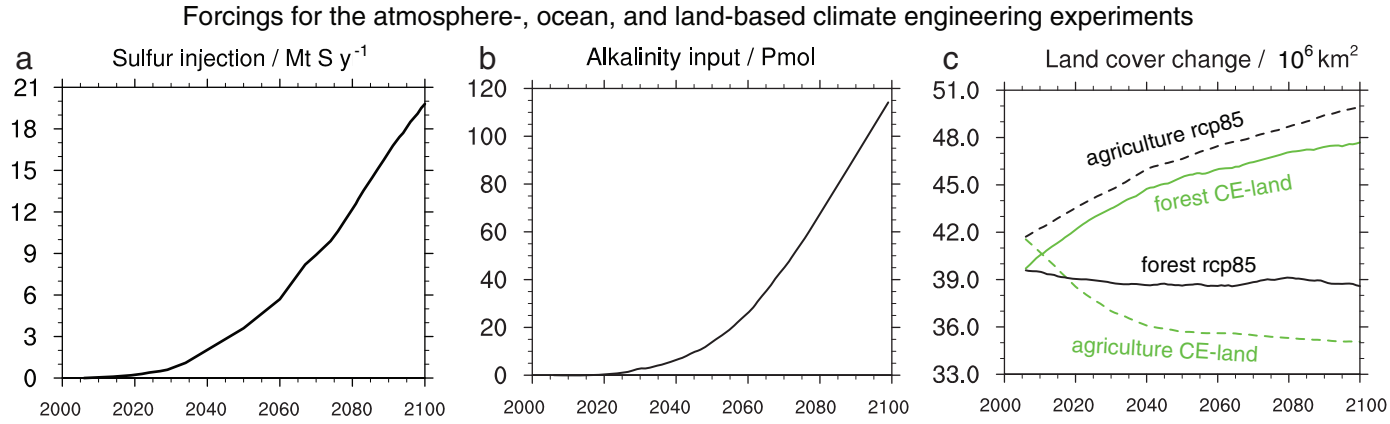

Figure 1. (a) Sulfur injections in experiment CE-atmos needed to reduce the radiative forcing from RCP8.5 to RCP4.5 levels, (b) alkalinity input in experiment CE-ocean needed to reduce the atmospheric CO_2 concentration to RCP4.5 levels, and (c) global annual mean agricultural (crops + pastures) areas and resulting forest areas in experiments rcp85 and CE-land for the years 2006–2100.

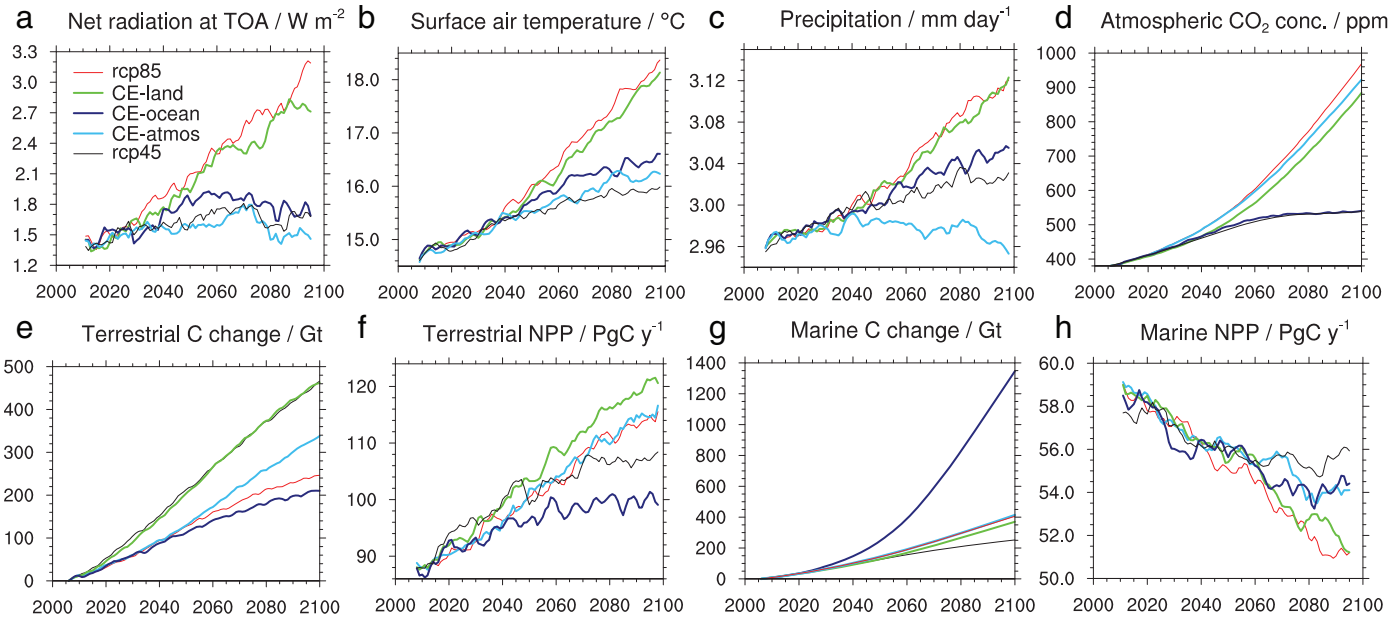

Figure 2. Global annual means of (a) net radiation at the top of the atmosphere (TOA), (b) surface air temperature, (c) precipitation, and (d) atmospheric CO_2 concentration. Annual means of total global (e) terrestrial carbon content change, (f) terrestrial net primary productivity (NPP), (g) marine (ocean + sediment) carbon content change, and (h) marine NPP in experiments rcp85, CE-atmos, CE-land, CE-ocean, and rcp45 for the years 2006–2100. The plots show 5-year running means for (b), (c), and (f) and 11-year running means for (a) and (h).

surface air temperature of the coldest night of a year between CE-atmos and rcp85 (Figure 3c) is similar to the one of the annual mean difference, but has a slightly higher amplitude.

Global warming is expected to amplify the hydrological cycle with global mean precipitation being strongly increased in a warmer climate (Held & Soden, 2006). Earlier observational and model studies have indicated potential impacts of SRM on the hydrological cycle (Robock et al., 2008; Trenberth & Dai, 2007), which we also find in our simulations: the global mean precipitation is much lower in CE-atmos than in rcp85 and in rcp45 (Figure 2c). This finding is in line with previous model studies that found that SRM decreases global mean precipitation (Bala et al., 2008; Kravitz et al., 2013a; Schmidt et al., 2012; Tilmes et al., 2013) and that this decrease is particularly strong for aerosol-based methods compared to space-based mirrors (Niemeier et al., 2013). As described in Schmidt et al. (2012) the weakening of the hydrological cycle can be explained by the fact that the solar forcing acts primarily on the surface, while CO_2 acts on the whole

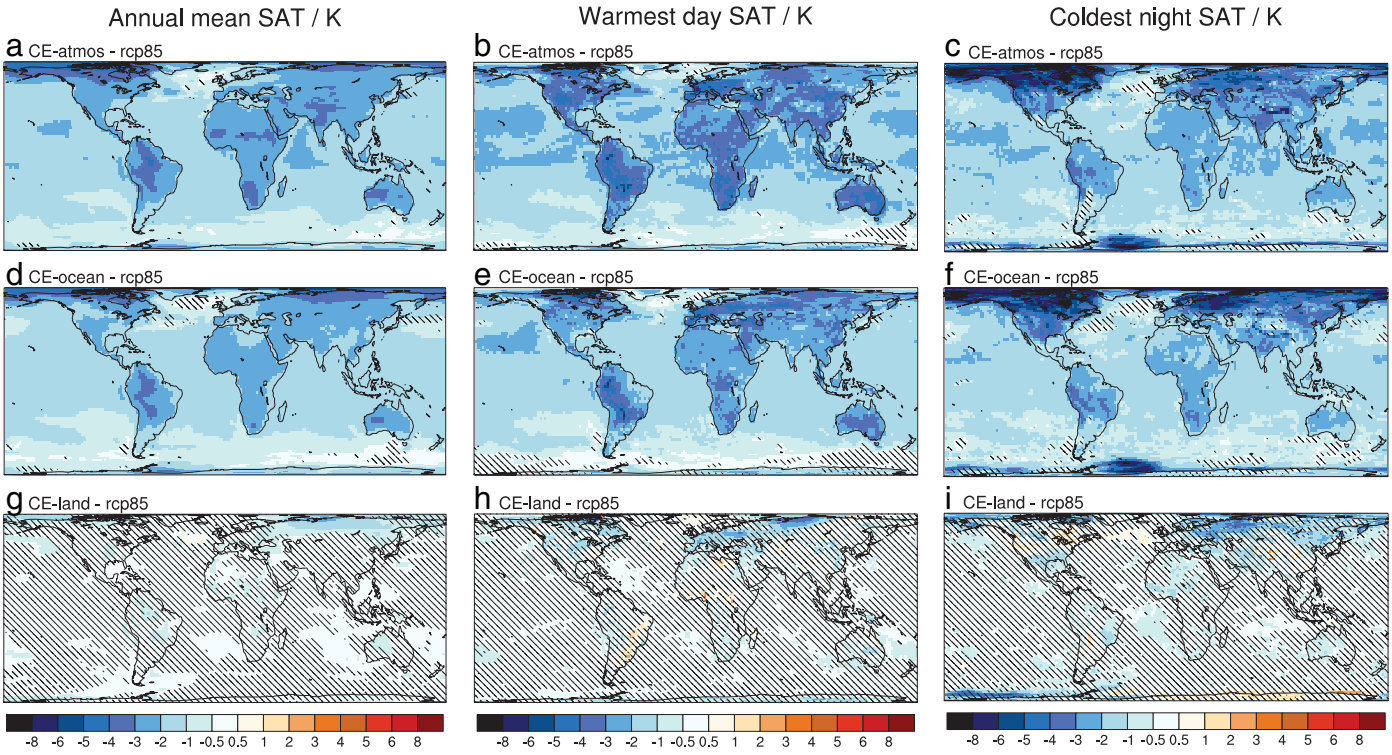

Figure 3. Multiannual (2081–2100) mean surface air temperature (SAT) differences between experiments CE-atmos and rcp85 for (a) the annual mean, (b) the warmest day, and (c) the coldest night of a year. The corresponding differences are shown in (d), (e), and (f) for CE-ocean and (g), (h), and (i) for CE-land. Differences that are not significant at the 5% level are indicated by hatched areas. Significance is calculated using a Student's *t* test modified to account for temporal autocorrelation (Zwiers & von Storch, 1995).

troposphere. This reduction in surface shortwave forcing leads to a reduction of the latent heat flux and thus to a reduction of precipitation to close the surface energy budget. The precipitation decrease by SRM is simulated in most mid to high latitude regions, while in the tropics and subtropics some regions show a strong decrease and others show a strong increase in precipitation (Figure 4a), which is in agreement with earlier studies (Schmidt et al., 2012). Although precipitation alone has been proven insufficient for a comprehensive hydrological assessment of SRM in earlier studies (e.g., Kravitz et al., 2013a; Schmidt et al., 2012), we find a similar spatial pattern and magnitude for the difference between precipitation and evaporation as for precipitation (Figures 4a and 4b).

Since MPI-ESM includes a fully coupled carbon cycle and our model experiments are driven by fossil-fuel CO_2 emissions, atmospheric CO_2 is calculated prognostically and is affected by the simulated CE methods. By definition of "CDR," reforestation and ocean alkalinization target at a decrease of atmospheric CO_2; however, also SRM is found to have substantial impacts on CO_2: atmospheric CO_2 concentration is reduced by 46 ppm in the global annual mean in CE-atmos compared to rcp85 by the year 2100 (Figure 2d). Such a reduction due to SRM has also been found in earlier studies that used an Earth system model of intermediate complexity and highly idealized representations of SRM. In those studies the reduction of atmospheric CO_2 was attributed to a general enhancement of natural (land and ocean) carbon sinks due to lower temperatures (Matthews & Caldeira, 2007) or more specifically to an enhanced terrestrial carbon sink due to higher primary productivity and lower soil carbon loss via heterotrophic respiration as a result of lower temperatures (Keller et al., 2014; Matthews et al., 2009).

In our model experiment we also find an enhanced terrestrial carbon sink with 92 Gt more land carbon in CE-atmos than in rcp85 by the year 2100 (Figure 2e). However, the increase in global terrestrial NPP over the century is comparable in these two experiments (Figure 2f) and the difference in land carbon is largely due to a stronger increase in soil carbon in CE-atmos compared to rcp85 (Figure 5). The comparable land NPP in the two experiments can be explained by compensating effects: lower temperatures in CE-atmos lead to weaker boreal forest expansion and thus lower NPP in mid to high latitudes (Figure 6a), while in several

Table 2.
Overview of the Simulated Climate Engineering (CE) Effects on Global Annual Mean Values of Surface Air Temperature, Precipitation, Atmospheric CO_2 Concentration, and Global Carbon Inventories

	Present	rcp85 difference to present	rcp45	CE-atmos	CE-ocean	CE-land
			Difference to rcp85			
Surface air temperature (K)	287.43	3.73	−2.10	−1.83	−1.55	−0.27
Precipitation (mm d^{-1})	2.94	0.18	−0.08	−0.14	−0.06	−0.01
Atmospheric CO_2 conc. (ppm)	380	589	−430	−46	−430	−85
Carbon content (Gt)						
Atmosphere	805	1246	−911	−100	−905	−180
Ocean	42,642	406	−154	8	941	−36
Land	3404	246	220	92	−36	216

Note. "Present" refers to multiannual means of experiment hist for the years 1986–2005 for temperature and precipitation and to annual means of experiment rcp85 in the year 2006 for CO_2 and the carbon pools. The differences are calculated for multiannual means for the years 2081–2100 for temperature and precipitation and annual mean values in the year 2100 for CO_2 and the carbon pools. The differences are significant at the 5% level according to a Student's *t* test modified to account for temporal autocorrelation (Zwiers & von Storch, 1995).

tropical and subtropical regions higher water availability (see Figure 4a) leads to higher NPP (Figure 6a) in CE-atmos compared to rcp85. In comparison to experiment rcp45, the terrestrial carbon content is much lower in CE-atmos despite higher CO_2 concentration, because the global forest area is much larger in rcp45 than in CE-atmos due to the different land-use forcings (afforestation in rcp45, deforestation in CE-atmos).

The response of terrestrial NPP to SRM has been found to be sensitive to the inclusion of a nitrogen cycle in models (Glienke et al., 2015). Since this sensitivity is due to the CO_2 fertilization effect that is overestimated without inclusion of nitrogen, this indicates that the increased NPP in experiment CE-atmos compared to rcp45 may be overestimated. Yet, the difference in NPP between CE-atmos and rcp85 may not be affected much, as the difference in the CO_2 concentrations is not large. Xia et al. (2016) find enhanced simulated plant photosynthesis rates in response to stratospheric aerosols and partly attribute this to enhanced diffuse radiation. We also find increased diffuse radiation in experiment CE-atmos compared to rcp85 (not shown), which is partly due to stratospheric aerosols, but also due to changes in clouds. The marine contribution to the carbon sink in our SRM experiment is only minor compared to the terrestrial contribution, with the total marine (ocean and sediment) carbon content being higher by 8 Gt in CE-atmos than in rcp85 by the year 2100 (Figure 2g). This increase in marine carbon can partly be attributed to the weaker decline in global marine NPP in CE-atmos compared to rcp85 over the century (Figure 2h), which can be explained by the weaker warming that leads to less stratification of the upper ocean and thus to a weaker decline of nutrient supply from deeper levels. Other factors leading to an increased oceanic carbon sink in CE-atmos compared to rcp85 are the enhanced CO_2 solubility in colder sea water and the weaker reduction of the Atlantic meridional overturning circulation (not shown), as has been discussed by Tjiputra et al. (2016) and Hong et al. (2017).

Tjiputra et al. (2016) use a similar model setup (ESM of comparable complexity and similar experimental setup) and find a much weaker effect of stratospheric aerosol enhancement on atmospheric CO_2 than we do, even in an experiment with a net radiative forcing that is stronger than the one in our SRM experiment. These different net responses of CO_2 to SRM may be due to differences in the ESMs and differences in the details of the CO_2 forcings (CO_2 emissions due to land-use changes are prescribed in Tjiputra et al. (2016), whereas they are calculated prognostically in our setup). Tjiputra et al. (2016) argue that in their model experiment the comparatively small CO_2 response to SRM is due to the small land carbon response because of nitrogen limitation, while in previous studies the higher CO_2 response was partly due to the missing nitrogen coupling. Yet, as described above, in our experiment the land carbon uptake is increased due to increased soil carbon because of reduced temperatures and thus reduced soil respiration, while NPP is almost unchanged in response to SRM. It is, however, possible that nitrogen limitation would be enhanced with reduced soil respiration and thereby reduce NPP.

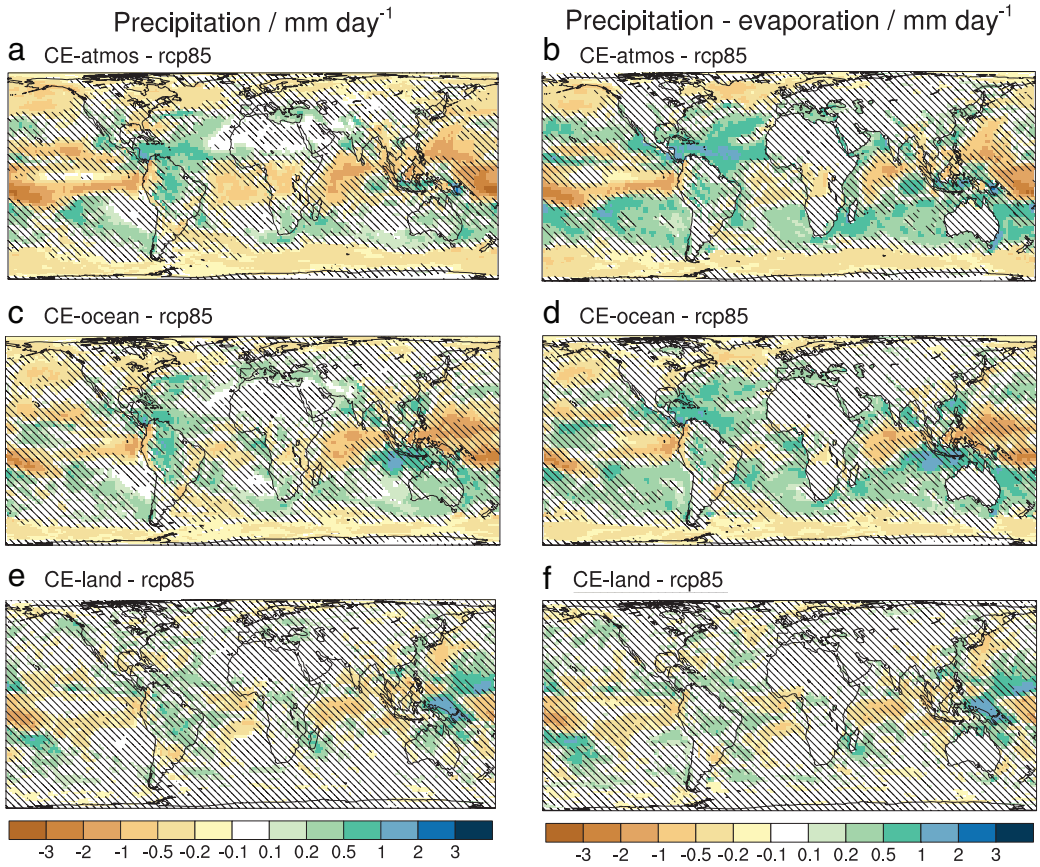

Figure 4. Multiannual (2081–2100) mean differences for precipitation in (a), (c), and (e) and for the difference between precipitation and evaporation in (b), (d), and (f) between experiments CE-atmos, CE-ocean, and CE-land and experiment rcp85. Significance is calculated using a Student's *t* test modified to account for temporal autocorrelation (Zwiers & von Storch, 1995).

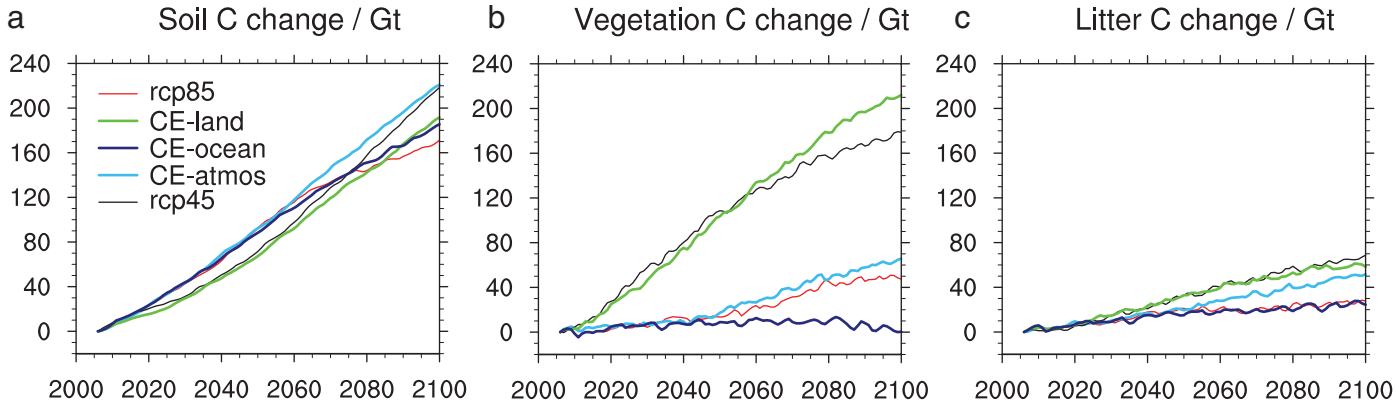

Figure 5. Total global annual mean carbon content change in the (a) soil, (b) vegetation, and (c) litter pools in experiments rcp85, CE-land, CE-ocean, CE-atmos, and rcp45 for the years 2006–2100.

Furthermore, Tjiputra et al. (2016) find that the marine carbon sink is enhanced in their SRM experiment while the terrestrial carbon sink shows little response. They attribute this dominant contribution of the marine carbon sink to the fact that their model shows a small sensitivity of the land carbon uptake to changes in climate and CO_2. Since the ocean and land carbon sinks both depend on and affect atmospheric CO_2, in models with a low sensitivity of the land carbon uptake to changes in climate and CO_2 the ocean carbon sink will be affected more strongly by SRM, and vice versa. Consistently, in our study, we find that

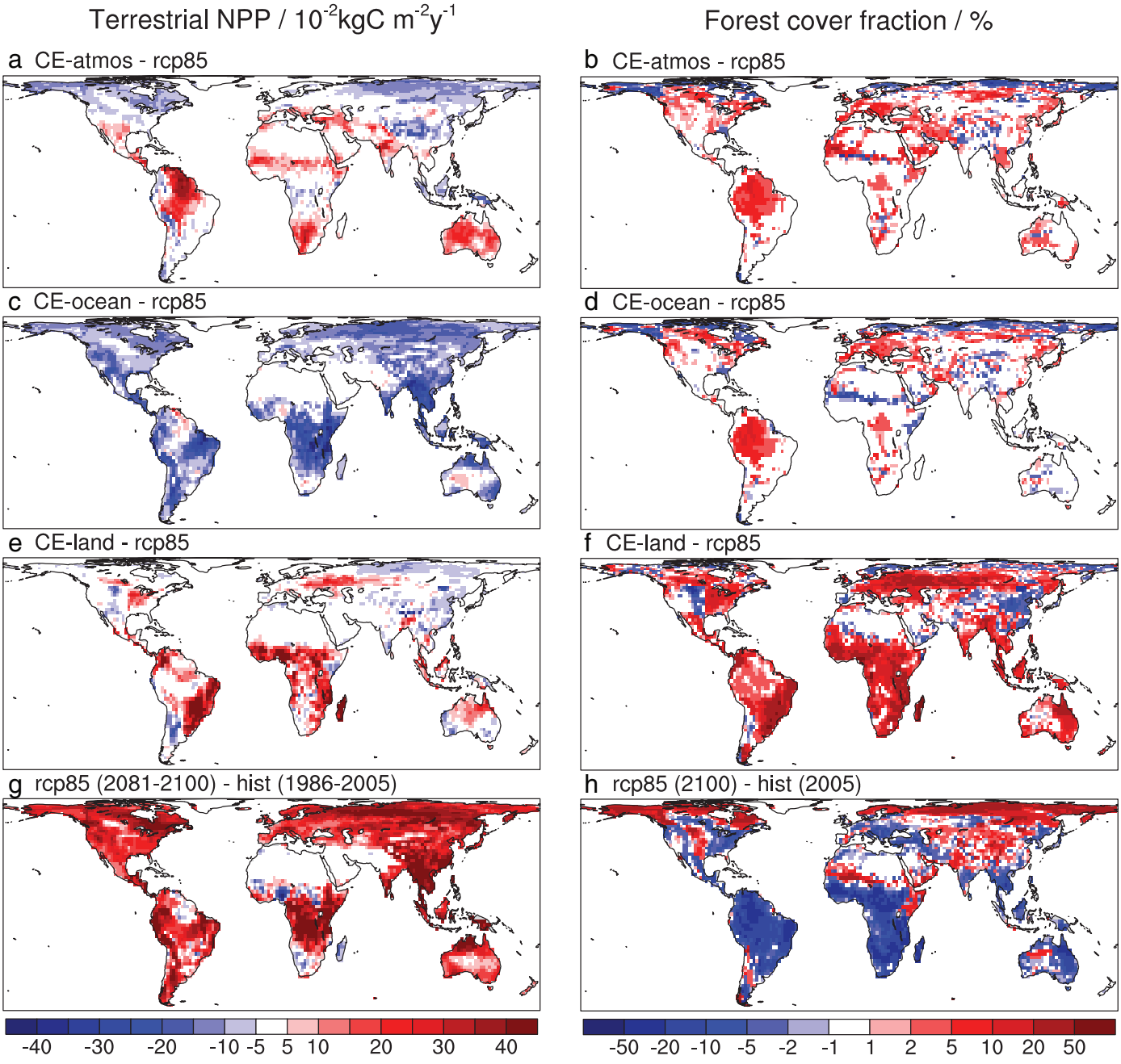

Figure 6. Multiannual (2081–2100) mean difference of terrestrial net primary productivity (NPP) between experiments (a) CE-atmos, (c) CE-ocean, and (e) CE-land and rcp85, and (g) between rcp85 and the multiannual (1986–2005) mean of experiment hist, and annual (2100) mean difference of forest cover fraction between experiments (b) CE-atmos, (d) CE-ocean, and (f) CE-land and rcp85, and (h) between rcp85 and the 2005 mean of experiment hist.

the ocean carbon sink will be affected less strongly, since our model shows higher sensitivity of the land carbon uptake to changes in climate and CO_2. These findings suggest that better constraints of this carbon uptake sensitivity are needed.

3.1.2. Ocean Alkalinization

As a CDR method, ocean alkalinization aims at enhancing the natural process of weathering and thereby increasing CO_2 sequestration (e.g., Hartmann et al., 2013; Renforth & Henderson, 2017). In our model experiment CE-ocean the cumulative alkalinity input increases drastically with increasing fossil-fuel CO_2

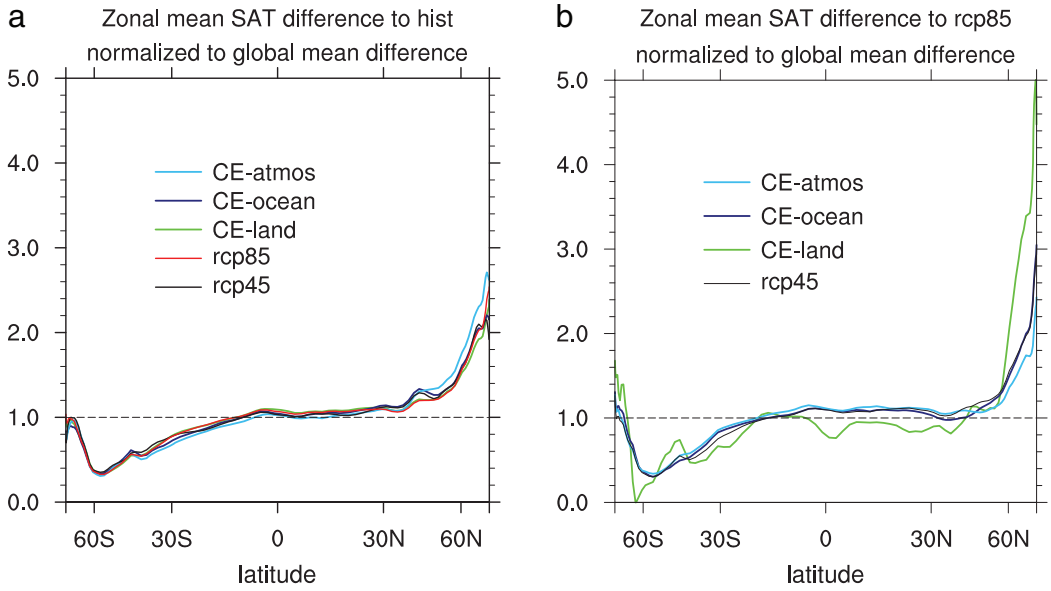

Figure 7. Zonal mean differences of the multiannual (2081–2100) mean surface air temperature (SAT) of experiments CE-atmos, CE-ocean, CE-land, rcp85, and rcp45 (a) to the 1985–2005 mean of experiment hist and (b) to the 2081–2100 mean of experiment rcp85, normalized to the respective global mean difference.

emissions over the century and amounts to about 114 Pmol of alkalinity by the year 2100 (Figure 1b). As explained in Ferrer González and Ilyina (2016) about 4010 Gt of olivine or 4220 Gt of lime would be needed for this alkalinity increase, requiring an increase of three (two) orders of magnitude in the total olivine (lime) production until 2100.

By construction of the experiment, the CO_2 concentration in CE-ocean closely follows that of experiment rcp45 (Figure 2d). As expected, the CDR in CE-ocean leads to a weakening of the anthropogenic global warming (Figure 2b), with a global mean cooling of 1.55 K averaged over the years 2081–2100 compared to rcp85 (Table 2). This cooling as well as all other effects on the climate in this experiment is exclusively due to the reduction of CO_2, since in the model there is no interactive feedback from ocean biogeochemistry to the climate other than via CO_2. The spatial pattern of this cooling is similar to the one in experiment CE-atmos, with more pronounced cooling in the Arctic and more pronounced cooling over land than over ocean (Figure 3d). The global annual mean temperature in CE-ocean is higher by 0.55 K averaged over the years 2081–2100 compared to rcp45. This difference can be attributed to the forcings of non-CO_2 greenhouse gases, of aerosols, and of biogeophysical effects from different land cover due to land-use transitions that are all taken according to RCP8.5 in CE-ocean, but according to RCP4.5 in experiment rcp45. The CO_2 emissions due to land-use changes are compensated already in CE-ocean. By simulation design in CE-atmos not only the CO_2 forcing, but all anthropogenic forcings of RCP8.5 are counterbalanced to follow the radiative forcing as in RCP4.5.

The simulated effects of ocean alkalinization on temperature extremes are similar as those in the SRM experiment: the multiannual mean surface air temperature difference of the warmest day of a year between CE-ocean and rcp85 is more pronounced over land compared to sea than the annual mean (Figure 3e), whereas the Arctic amplification of the signal is stronger for the annual mean difference (Figure 3d). Also the spatial pattern of the multiannual mean surface air temperature difference of the coldest night of a year between CE-ocean and rcp85 (Figure 3c) is similar to the one of the annual mean difference, but has a slightly higher amplitude.

The differences in the global mean greenhouse-gas forcings are also reflected in the net radiation at the top of the atmosphere that increases much less strongly over the century in CE-ocean than in rcp85 and slightly more strongly compared to rcp45 (Figure 2a). Also global mean precipitation shows a similar response as global mean temperature: the increase in global mean precipitation over the century is much weaker in CE-ocean than in rcp85 and slightly stronger than in rcp45 (Figure 2c). While the global mean decrease

of precipitation compared to rcp85 is less strong in CE-ocean than in CE-atmos, the spatial patterns of the precipitation differences are similar, with a consistent drying of mid to high latitudes, but regions with strong increase and strong decrease in precipitation in the tropics (Figure 4c). As for CE-atmos, we find a similar spatial pattern and magnitude for the difference between precipitation and evaporation as for precipitation (Figures 4c and 4d). Although in large areas the signals are not significant, this indicates that both CDR and SRM may have strong impacts on hydrology and that this is not an exclusive feature or risk of SRM as has been suggested (e.g., Royal Society, 2009). Also, the discussed climate effects are all in line with what could be expected for a reduction in CO_2 and are not specific to the CE method of ocean alkalinization.

Due to the increased buffering capacity of the ocean and facilitated by colder sea water in the alkalinization experiment the marine carbon uptake increases strongly, with the marine carbon content being 941 Gt higher in CE-ocean than in rcp85 by the year 2100 (Figure 2g). While the increases in carbon stocks over the century are 1246, 406, and 246 Gt in atmosphere, ocean, and land, respectively, in experiment rcp85, they are 341, 1347, and 210 Gt in CE-ocean. As a response to the weaker warming over the century due to alkalinization, the decline of the marine NPP is also weakened in CE-ocean compared to rcp85 (Figure 2h), which can be explained by a weaker increase in stratification leading to a less strong suppression of nutrient supply to the surface ocean.

The changes in climate and atmospheric CO_2 due to alkalinization also affect the terrestrial carbon sink. The effect is less strong than in the SRM experiment and in the opposite direction: the total terrestrial carbon content is lower by 33 Gt in CE-ocean than in rcp85 by the year 2100 (Figure 2e). While the soil carbon content is higher in CE-ocean due to lower temperatures and thus lower soil respiration in CE-ocean than in rcp85, the vegetation carbon content is lower by 50 Gt by the year 2100 (Figure 5), overcompensating the soil carbon content increase. The lower vegetation carbon content and the weaker increase in terrestrial NPP (Figure 2f) in CE-ocean compared to rcp85 can be explained by the much lower CO_2 concentration leading to weaker CO_2 fertilization and by the lower temperature leading to weaker boreal forest expansion compared to rcp85.

The substantially lower terrestrial carbon content and NPP in CE-ocean compared to rcp45 (Figures 2e and 2f) despite only minor differences in the global mean climate and atmospheric CO_2 between these two experiments can largely be explained by the different land-use forcings (deforestation in CE-ocean, afforestation in rcp45), which lead to much less forest in CE-ocean.

Ferrer González and Ilyina (2016) showed that the global marine biogeochemical effects of ocean alkalinization in CE-ocean are consistent with results of previous model studies using different model setups and different alkalinization scenarios (Ilyina et al., 2013a, 2013b; Keller et al., 2014; Köhler et al., 2013). However, there are fewer studies to compare the effects of ocean alkalinization on the climate system and the global carbon cycle. Using an Earth system model of intermediate complexity, Keller et al. (2014) also find a reduction of atmospheric CO_2 and consequently a global cooling effect due to ocean alkalinization. They also find an increase in the ocean carbon content and a slight decrease in the terrestrial carbon content in their ocean alkalinization experiment. Yet, the effects are all smaller in magnitude, since in their study the amount of added alkalinity was smaller and thus the results are not directly comparable in a quantitative manner.

3.1.3. Reforestation

The large-scale abandonment of agricultural areas in the RCP4.5 land-use scenario that is used in experiment CE-land leads to an increase in global forest area by about 8 million km^2 over the 21st century, while it decreases by about 1 million km^2 in rcp85 (Figure 1c). The increase in global forest cover in CE-land leads to a stronger increase of terrestrial carbon (Figure 2e) and to a weaker increase in atmospheric CO_2 (Figure 2d) over the course of the century. By the year 2100, the land carbon content is 215 Gt higher and the atmospheric CO_2 concentration is 85 ppm lower in CE-land compared to rcp85. This CDR potential of reforestation is higher than previous estimates (e.g., House et al., 2002) and is due to increased forest cover in combination with enhanced terrestrial carbon uptake in a warm and high-CO_2 climate, suggesting that the CDR potential of reforestation depends on the background state of the Earth system (Sonntag et al., 2016). The CDR potential may be lower in a model including nitrogen limitation, as demonstrated recently by Kracher (2017). Yet, the study by Kracher (2017) used a different baseline climate (RCP4.5 instead of RCP8.5) and found a large effect mostly on boreal forest expansion, which makes a quantitative estimate of the effect of nitrogen in our scenario difficult. Terrestrial carbon is very similar in experiments rcp45 and CE-land (Figure 2e),

because of two compensating effects: a decrease in soil carbon due to weaker soil respiration because of lower temperatures and an increase in vegetation carbon in CE-land compared to rcp45 (Figure 5b).

In response to the reduction in atmospheric CO_2 concentration and to the changes in land cover in CE-land, the net radiation at the top of the atmosphere increases slightly less strongly over the century in CE-land than in rcp85 (Figure 2a). The global mean temperature is reduced by 0.27 K averaged over the years 2081–2100 (Figure 2b and Table 2) with the most pronounced cooling in the Arctic (Figure 3g). The net effect being a cooling suggests that globally the cooling CDR effect dominates over the warming biogeophysical effect that a forest increase has in particular in boreal regions due to an increase in surface albedo (e.g., Bonan et al., 1992). Previous idealized model studies on large-scale afforestation suggested that the albedo warming dominates over the CDR cooling in boreal regions (Bathiany et al., 2010; Claussen et al., 2001; Sitch et al., 2005), whereas other studies indicate that afforestation can lead to a global warming when applied in the Saharan and Australian deserts (Keller et al., 2014; Ornstein et al., 2009). In our experiment CE-land, the net global effect of reforestation is a cooling, since forest regrowth occurs on previously cleared land for agricultural use. This land was picked for agriculture earlier because it was more productive and had little snow. Thus, forests that regrow on these areas have a stronger cooling CO_2 and a weaker warming snow-masking effect (Pongratz et al., 2011).

The spatial patterns of the surface air cooling signal of reforestation are similar for the annual mean, for the warmest day, and the coldest night of the year, but the amplitude of the signal is stronger for the coldest night than for the annual mean (Figure 3i). Furthermore, as also shown in Sonntag et al. (2016), the cooling is more pronounced in the mid-northern latitudes for the warmest day than for the annual mean (Figure 3h), suggesting a reduction in extremely warm days due to reforestation in this region.

The increase in global mean precipitation is very similar in CE-land and rcp85 (Figure 2c), indicating that the net global effect of the CDR and the change in land cover on precipitation is small in this scenario. Also, in most areas the difference in precipitation and in the difference between precipitation and evaporation between CE-land and rcp85 is not significant (Figures 4e and 4f).

Global terrestrial NPP increases more strongly over the century in CE-land than in rcp85 (Figure 2f) since the differences in temperature, precipitation, and CO_2 between these two experiments are not large, but the global forest area is much larger in CE-land than in rcp85 (Figure 1c). Global marine NPP decreases slightly less strongly over the century in CE-land than in rcp85 (Figure 2h), which may be explained by less warming leading to a weaker increase in thermal stratification of the ocean and thus weaker decrease of nutrient supply to the surface. Despite this slight relative enhancement of the marine NPP and the cooling due to reforestation, the marine carbon sink is weakened with 36 Gt carbon less in CE-land than in rcp85 by the year 2100 (Figure 2g). This weakening of the marine carbon sink is due to the reduction of the atmospheric CO_2 concentration leading to a smaller air-sea CO_2 gradient in CE-land compared to rcp85.

3.2. Comparison of CE Methods

The three CE methods differ vastly in their simulated effects on the Earth system. In terms of reducing future global mean warming in our simulations, SRM has the largest effect, ocean alkalinization is only slightly weaker, since it does not act on the non-CO_2 forcings as opposed to SRM, and reforestation has a relatively small effect (Figure 2b). Also regarding global mean precipitation, SRM has by far the largest effect relative to the rcp85 baseline simulation, ocean alkalinization has a weaker effect, and reforestation has a minor effect (Figure 2c). In terms of atmospheric CO_2, however, the situation is different: ocean alkalinization has the largest effect, reforestation has a much smaller effect, and SRM has an even smaller effect (Figure 2d). Concerning global terrestrial NPP, we see yet a different picture: ocean alkalinization is simulated to have the largest effect, reforestation has a weaker effect, but in the opposite direction, and SRM has almost no effect (Figure 2f) compared to the rcp85 baseline simulation.

3.2.1. Reasons for Different CE Effects

The differences in the effects of the CE methods on the Earth system are mainly due to the different radiative forcings in the experiments. The differences are also due to different target processes invoked by the methods: SRM targets the short-wave radiative forcing and aims at reducing temperature by reducing the incoming solar radiation, whereas CDR methods target the land or ocean carbon sinks and aim at reducing temperature by reducing absorption of long-wave radiation by CO_2 in the atmosphere. And since the

methods have these different targets, different effects may be regarded as intended or unintended: while changes in carbon are intended for CDR methods, they may be unintended for SRM.

In addition to the fundamentally different targets and underlying mechanisms of the different CE methods, their effects on the Earth system also depend very much on how the CE scenarios are designed. In CE-atmos the net radiative forcing and in CE-ocean the atmospheric CO_2 concentration are prescribed, whereas in CE-land the model input in terms of land-use transitions instead of a target quantity is prescribed. By construction of the three CE experiments, the resulting radiative forcings and thus also, for example, the resulting temperature changes due to CE, are of comparable magnitude for CE-atmos and CE-ocean, but much smaller for CE-land.

Using a simpler Earth system model of intermediate complexity, Keller et al. (2014) compared the effects of different CE methods within one Earth system model. Although they studied similar CE methods, the results are not directly comparable to ours, since they used different scenarios of CE implementation and focused on assessing the maximum potentials of different CE methods. Whereas our SRM and ocean alkalinization scenarios target the RCP4.5 radiative forcing and CO_2 concentration, respectively, and our reforestation scenario is based on the RCP4.5 land-use transitions, in Keller et al. (2014) the target quantity for SRM was preindustrial global mean surface air temperature, the ocean alkalinization intensity was set by an estimate for the technical limit, and the afforestation scenario was based on large-scale irrigation of deserts.

The simulated effects of CE methods on the Earth system also depend on the model that is used for the simulations. For example, as discussed earlier, the effect of SRM on CO_2 depends on the interaction of several model components and varies from one ESM to another. The Earth system model used in Keller et al. (2014), for example, includes an energy-moisture balance model as opposed to a full atmospheric general circulation model in MPI-ESM, and different model components for the ocean, the land surface, and the carbon cycle.

Furthermore, as discussed above in the rankings of the CE methods, the choice of variables that are considered in the analysis plays a crucial role in the assessment of CE methods (Oschlies et al., 2016).

3.2.2. Evaluation of Normalized Effects

To allow for a better comparison of the three CE methods, we normalize the CE effects to a reference change. First, we normalize the surface air temperature (SAT) differences both between the experiments at the end of the century (years 2081–2100) and the end of the historical period (years 1986–2005 of experiment hist) and between the experiments and the reference experiment rcp85 at the end of the century to the respective global mean differences. Second, we normalize the global mean precipitation difference between the experiments at the end of the century and at the end of the historical period to a change in global mean SAT of 1 K. And third, to compare the CE effects on the carbon cycle, we normalize the differences in the atmosphere, ocean, and land carbon pools in the CE experiments to the reference experiment rcp85 to a global mean SAT difference of 1 K and to a difference in atmospheric CO_2 concentration of 100 ppm.

As shown before, the SAT differences of the experiments CE-atmos and CE-ocean to rcp85 are substantially larger than that of CE-land in most regions of the world (see Figures 3a, 3d and 3g). The corresponding normalized differences, however, are similar (Figure 7a). Also the spatial patterns of the normalized warming (i.e., the normalized SAT differences to the historical period) are very similar (not shown). This suggests that the local amplification factor compared to the global mean SAT change over the century is robust across the CE scenarios, which has also been found for different RCP scenarios simulated with MPI-ESM (Giorgetta et al., 2013). Despite these similarities, for the RCP scenarios slightly less Arctic amplification for scenarios with stronger forcing has been found (Giorgetta et al., 2013), presumably partly because under strong warming Arctic sea ice is reduced so much that the sea ice albedo feedback is weakened. We can reproduce this finding with respect to CE-ocean, which shows similar amplification as rcp45 and slightly stronger amplification than rcp85 (Figure 7a). However, CE-land shows slightly lower amplification than rcp85 despite smaller forcing. Experiment CE-atmos, on the other hand, shows a larger Arctic amplification than all other experiments despite comparable forcing to rcp45 and CE-ocean. When comparing the normalized SAT differences to the reference experiment rcp85 at the end of the century rather than to the historical period, we see a similar picture: the general zonal patterns of the differences are similar to each other, whereas the Arctic cooling signal due to CE is dampened in CE-atmos, but amplified in CE-land (Figure 7b). This amplified

Table 3.
Global Carbon Content Differences in the Climate Engineering (CE) Experiments Compared to Experiment rcp85 in the Year 2100, Normalized to a Difference in Global Mean Surface Air Temperature (SAT) of 1 K and in Atmospheric CO_2 Concentration of 100 ppm

Carbon content difference	CE-atmos	CE-ocean	CE-land
Normalized by SAT (Gt K^{-1})			
Atmosphere	−55	−584	−667
Ocean	4	607	−133
Land	51	−23	800
Normalized by CO_2 (10^{-2} Gt ppm^{-1})			
Atmosphere	−217	−210	−212
Ocean	17	219	−42
Land	200	−8	254

Note. The values for the atmospheric carbon content normalized to atmospheric CO_2 differ slightly for the three CE experiments, since the carbon mass is calculated for the whole atmosphere and normalized by the CO_2 concentration at the surface.

cooling in CE-land is due to the reduced forest cover in the very high Northern latitudes compared to rcp85 (Figure 6) in response to reduced warming in CE-land compared to rcp85 that leads to even less warming via snow-masking. This suggests that reforestation as simulated in our scenario has the potential to mitigate Arctic warming disproportionately.

Although the global mean precipitation change over the century is more than 50% larger in CE-land than in CE-ocean (see Figure 2c), these changes are very similar when normalized to the changes in global mean surface air temperature: The hydrological sensitivity, that is, the relative change in global mean precipitation per unit of global mean surface air temperature, is similar for CE-ocean (1.70%), CE-land (1.67%), and also rcp85 (1.64%), with values are typical for experiments with CO_2 forcings of these magnitudes (e.g., Giorgetta et al., 2013). For CE-atmos, the hydrological sensitivity is smaller by a factor of three (0.54%). Our finding are also in agreement with previous studies that found that the hydrological sensitivity to solar forcing is higher than that due to CO_2 forcing by a factor of 1.5–2 (e.g., Bala et al., 2008). Using this definition of hydrological sensitivity involving the difference in precipitation per difference in temperature with respect to an unmitigated high-CO_2 scenario, which is rcp85 in our case, the hydrological sensitivity in our experiments is 2.45% for CE-atmos, 1.24% for CE-ocean, 1.19% for CE-land, and 1.22% for rcp45. For CE-ocean and CE-land the global hydrological sensitivities are similar despite the different patterns in temperature and precipitation. These findings suggest that the hydrological sensitivity of the Earth system is altered substantially by SRM, but only marginally by CDR methods.

The differences in the atmosphere, ocean, and land carbon pools to the reference experiment rcp85 differ vastly among the CE experiments (see Table 2). Normalization of these differences to reference changes in temperature and CO_2, respectively, highlights the effects that are specific to the different CE methods by eliminating the effects that are due to the strength of the CE scenarios in terms of their effects on temperature or CO_2. In the nonnormalized quantities the effect on atmospheric carbon is by far strongest in CE-ocean, whereas the CDR effect is strongest in CE-land when normalized to the change in temperature (Table 3). This means that in our simulations, to achieve the same reduction in global warming, more carbon needs to be removed from the atmosphere by reforestation (667 Gt C K^{-1}) than by ocean alkalinization (584 Gt C K^{-1}). This lower cooling efficiency of reforestation can be explained by warming regional biogeophysical effects counteracting the cooling signal of terrestrial CDR and is reflected in a slight decrease of the global mean surface albedo of 0.1% for the multi-year (2081–2100) mean difference between rcp85 and CE-land. Another factor playing a role in the different efficiencies of the two CDR methods is the nonlinear relationship between atmospheric CO_2 and temperature, since both CO_2 and climate are very different in CE-land and CE-ocean.

Furthermore, we find that, to achieve the same reduction in atmospheric CO_2, more carbon needs to be stored on land (2.54 GtC ppm^{-1}) in the reforestation scenario than in the ocean (2.19 GtC ppm^{-1}) in the

alkalinization scenario (Table 3). This different efficiency to remove carbon from the atmosphere is due to the different compensation of the ocean releasing more carbon (0.42 GtC ppm^{-1}) in CE-land and of the land biosphere releasing relatively little carbon (0.08 GtC ppm^{-1}) in CE-ocean. These differences in the weakening of the CDR effect of about 17% in CE-land, but only about 4% in CE-ocean suggest that the ocean reacts more strongly to changes in atmospheric carbon than the land biosphere on the timescale of a century.

The effects on atmospheric and oceanic carbon are weakest in CE-atmos in the nonnormalized quantities and are even weaker compared to CE-land and CE-ocean when normalized to the change in temperature (Table 3). The effect on land carbon in CE-atmos is smaller than the one in CE-land and is even smaller when normalized to the temperature change. When normalized to the change in atmospheric CO_2 concentration, however, the effect on the land and ocean carbon pools in CE-atmos is of comparable magnitude than the one in CE-land, indicating that comparable reductions in atmospheric carbon would be accompanied by comparable increases in terrestrial carbon in these scenarios of SRM and reforestation. The effect on the oceanic carbon, normalized to the change in CO_2, however, is a slight increase in CE-atmos, but a decrease in CE-land.

4. Summary and Conclusion

Our results show that, driven by different target variables — reduction of atmospheric CO_2 for CE-land and CE-ocean, radiative forcing for CE-atmos — the different CE methods differ vastly in terms of their effects and feedbacks with different Earth system components. For example, we find:

- Despite different amounts of global surface cooling achieved, local amplification factors compared to the global mean temperature changes are generally similar in the CE scenarios. A notable difference exists with respect to Arctic amplification, which is strengthened in CE-atmos, slightly strengthened in CE-ocean, and slightly weakened in CE-land compared to the historical period.
- Effects on variables beyond global mean temperature are substantial: For example, global mean precipitation, as discussed in earlier studies, decreases stronger in CE-atmos than one may expect from a temperature reduction alone. That is, for CE-atmos the hydrological sensitivity is strongly reduced. As expected, the precipitation reduction and the hydrological sensitivity are similar for CE-ocean as for rcp45. Unintended effects may even influence the cooling efficiency of the CE method: Regional biogeophysical effects of afforestation leading to warming counteract the cooling signal due to reduced CO_2 radiative forcing of the terrestrial CDR, so that more carbon needs to be removed from the atmosphere in CE-land than in CE-ocean to achieve the same reduction in global warming.
- Similarly, effects on Earth system components not targeted by the CE method are found to be substantial: Global terrestrial NPP, which features a targeted increase in CE-land, is substantially reduced in CE-ocean, whereas in CE-atmos there is almost no net effect on global terrestrial NPP due to counteracting effects of decreased water stress in low latitudes and weaker boreal forest expansion. The ocean carbon sink is not just drastically increased in CE-ocean, but it is also increased in CE-atmos, whereas it is weakened in CE-land.
- Carbon cycle feedbacks in the coupled Earth system alter the mitigation potential of CE methods: In particular, the climate-carbon cycle feedback contributes to a larger mitigation potential in CE-atmos, where atmospheric CO_2 is reduced due to enhanced land carbon uptake under cooler conditions. Further, compensatory fluxes between land and ocean carbon reservoirs makes CE-ocean more efficient than CE-land, that is, less carbon needs to be stored in the ocean in the alkalinization scenario than on land in the reforestation scenario, as the ocean outgasses faster in response to terrestrial CDR than land does to oceanic CDR.

We also identify challenges when comparing the effects of the different CE methods on the Earth system. We illustrate that the scenario design already sets targets and potentials of the respective CE method and that the quantitative results depend on the details of the CE scenarios, on the type of model that is used for the simulations, and also on the choice of variables that are analyzed in an assessment of CE methods. Also, some of the responses are specific to the CE method under consideration, whereas others can be expected also for similar methods. For example, as the CO_2 reduction in CE-atmos is due the reduction in temperature, we can assume it would be similar for other SRM methods. On the other hand, it has been shown in (Niemeier et al., 2013) that precipitation responses may depend on the specific SRM method. Concerning the CDR

methods, in our study ocean alkalinization has effects on climate only via changes in CO_2, and hence these climate effects are typical for a CO_2 reduction, while afforestation has additional effects via physical changes in land cover. Furthermore, the effect of a CE method may depend on the background state of the Earth system, for example, the reforestation CDR potential depends on climate and CO_2, making a comparative assessment of CE even more challenging. We also show that normalizations allow for a better comparability of different CE methods which, although not all effects may scale linearly at all scales, can serve as a basis for comparative assessments of CE. Such normalizations could also be used more generally to assess effects of other scenarios that do not involve CE.

Furthermore, we find that using a more complex ESM gives similar information on the qualitative global mean response of the Earth system to different CE methods as a relatively simpler ESM of intermediate complexity (EMIC) as used in Keller et al. (2014). Yet, to quantitatively investigate some of the intended and unintended CE effects and especially their spatial patterns and statistics a more complex ESM is better suited, since natural variability and relevant feedbacks can be captured more adequately. For example, we can show that the spatial cooling patterns of annual mean changes are different across CE methods as compared to those of the warm extreme.

Comprehensive reports of CE like, for example, Royal Society (2009), have approached the assessment of CE, also in terms of effects and side effects, and have compared these indicators for different CE methods. Our study suggests that in such assessments one needs to keep in mind that the quantitative intended and unintended effects of a potential CE deployment are strongly influenced by the details of the deployment. To improve the value of such assessments for policy advice and decision making more quantitative studies, such as in coordinated model intercomparison projects like GeoMIP (Kravitz et al., 2015), LUMIP (Lawrence et al., 2016), and CDR-MIP (Keller et al., 2017) can make valuable contributions.

As the potentials of individual CE methods to reduce climate change may be either limited, in particular for land-based CE methods, or come with high risks and large unintended effects, individual CE methods may be applied, if at all, as part of a portfolio that comprises various CE methods, possibly in combination with mitigation and adaptation efforts (Klepper & Rickels, 2012; Victor, 2008). A logical next step is therefore to study portfolio scenarios that combine different CE methods and allow investigating potential interactions of the methods. Cao et al. (2017) study the simultaneous deployment of different SRM methods, but a combination of land-, ocean- and atmosphere-based CE is still missing.

Acknowledgments
We thank Johann Jungclaus and two anonymous reviewers for their valuable comments on this article. This work was supported by the German Research Foundation's Priority Program 1689 "Climate Engineering" (projects ComparCE, CE-Land, and CELARIT) and its Emmy Noether Program (PO 1751/1-1). Computational resources were made available by the German Climate Computing Center (DKRZ) through support from the German Federal Ministry of Education and Research (BMBF). Primary data and scripts used in the analysis and other supplementary information that may be useful in reproducing the authors' work are archived by the Max Planck Institute for Meteorology and can be obtained by contacting publications@mpimet.mpg.de.

References

Arora, V. K., Boer, G. J., Friedlingstein, P., Eby, M., Jones, C. D., Christian, J. R., … Wu, T. (2013). Carbon-concentration and carbon-climate feedbacks in CMIP5 Earth system models. *Journal of Climate*, *26*(15), 5289–5314. https://doi.org/10.1175/JCLI-D-12-00494.1

Aswathy, V. N., Boucher, O., Quaas, M., Niemeier, U., Muri, H., Mülmenstädt, J., & Quaas, J. (2015). Climate extremes in multi-model simulations of stratospheric aerosol and marine cloud brightening climate engineering. *Atmospheric Chemistry and Physics*, *15*(16), 9593–9610. https://doi.org/10.5194/acp-15-9593-2015

Bala, G., Duffy, P. B., & Taylor, K. E. (2008). Impact of geoengineering schemes on the global hydrological cycle. *Proceedings of the National Academy of Sciences of the United States of America*, *105*(22), 7664–7669. https://doi.org/10.1073/pnas.0711648105

Bathiany, S., Claussen, M., Brovkin, V., Raddatz, T., & Gayler, V. (2010). Combined biogeophysical and biogeochemical effects of large-scale forest cover changes in the MPI Earth system model. *Biogeosciences*, *7*(5), 1383–1399. https://doi.org/10.5194/bg-7-1383-2010

Bonan, G. B., Pollard, D., & Thompson, S. L. (1992). Effects of boreal forest vegetation on global climate. *Nature*, *359*(6397), 716–718. https://doi.org/10.1038/359716a0

Boucher, O., Halloran, P. R., Burke, E. J., Doutriaux-Boucher, M., Jones, C. D., Lowe, J., … Wu, P. (2012). Reversibility in an Earth system model in response to CO_2 concentration changes. *Environmental Research Letters*, *7*(2), 024,013. https://doi.org/10.1088/1748-9326/7/2/024013

Brovkin, V., Boysen, L., Arora, V. K., Boisier, J. P., Cadule, P., Chini, L., … Weiss, M. (2013). Effect of anthropogenic land-use and land-cover changes on climate and land carbon storage in CMIP5 projections for the twenty-first century. *Journal of Climate*, *26*(18), 6859–6881. https://doi.org/10.1175/JCLI-D-12-00623.1

Budyko, M. I. (1977). *Climatic Changes* (p. 261). Washington, DC: American Geophysical Society. https://doi.org/10.1029/SP010

Caldeira, K., Bala, G., & Cao, L. (2013). The science of geoengineering. *Annual Review of Earth and Planetary Sciences*, *41*(1), 231–256. https://doi.org/10.1146/annurev-earth-042711-105548

Campbell, J. E., Berry, J. A., Seibt, U., Smith, S. J., Montzka, S. A., Launois, T., … Laine, M. (2017). Large historical growth in global terrestrial gross primary production. *Nature*, *544*(7648), 84–87. https://doi.org/10.1038/nature22030

Cao, L., & Caldeira, K. (2010). Atmospheric carbon dioxide removal: Long-term consequences and commitment. *Environmental Research Letters*, *5*(2), 024,011. https://doi.org/10.1088/1748-9326/5/2/024011

Cao, L., Duan, L., Bala, G., & Caldeira, K. (2017). Simultaneous stabilization of global temperature and precipitation through cocktail geoengineering. *Geophysical Research Letters*, *44*(14), 7429–7437. https://doi.org/10.1002/2017GL074281

Claussen, M., Brovkin, V., & Ganopolski, A. (2001). Biogeophysical versus biogeochemical feedbacks of large-scale land cover change. *Geophysical Research Letters*, *28*(6), 1011–1014. https://doi.org/10.1029/2000GL012471

Crutzen, P. J. (2006). Albedo enhancement by stratospheric sulfur injections: A contribution to resolve a policy dilemma? *Climatic Change*, *77*(3), 211–220. https://doi.org/10.1007/s10584-006-9101-y

Curry, C. L., Sillmann, J., Bronaugh, D., Alterskjaer, K., Cole, J. N. S., Ji, D., … Yang, S. (2014). A multimodel examination of climate extremes in an idealized geoengineering experiment. *Journal of Geophysical Research*, *119*(7), 3900–3923. https://doi.org/10.1002/2013JD020648

Davies-Barnard, T., Valdes, P. J., Singarayer, J. S., Wiltshire, A. J., & Jones, C. D. (2015). Quantifying the relative importance of land cover change from climate and land use in the representative concentration pathways. *Global Biogeochemical Cycles*, *29*(6), 842–853. https://doi.org/10.1002/2014GB004949

Erb, K.-H., Lauk, C., Kastner, T., Mayer, A., Theurl, M. C., & Haberl, H. (2016). Exploring the biophysical option space for feeding the world without deforestation. *Nature Communications*, *7*, 11382. https://doi.org/10.1038/ncomms11382

Ferrer González, M., & Ilyina, T. (2016). Impacts of artificial ocean alkalinization on the carbon cycle and climate in Earth system simulations. *Geophysical Research Letters*, *43*(12), 6493–6502. https://doi.org/10.1002/2016GL068576

Foley, J. A., Ramankutty, N., Brauman, K. A., Cassidy, E. S., Gerber, J. S., Johnston, M., … Zaks, D. P. M. (2011). Solutions for a cultivated planet. *Nature*, *478*(7369), 337–342. https://doi.org/10.1038/nature10452

Friedlingstein, P., Cox, P., Betts, R., Bopp, L., von Bloh, W., Brovkin, V., … Zeng, N. (2006). Climate-carbon cycle feedback analysis: Results from the C4MIP model intercomparison. *Journal of Climate*, *19*(14), 3337–3353. https://doi.org/10.1175/JCLI3800.1

Fuss, S., Jones, C. D., Kraxner, F., Peters, G. P., Smith, P., Tavoni, M., … Yamagata, Y. (2016). Research priorities for negative emissions. *Environmental Research Letters*, *11*(11), 115,007. https://doi.org/10.1088/1748-9326/11/11/115007

Gasser, T., Guivarch, C., Tachiiri, K., Jones, C. D., & Ciais, P. (2015). Negative emissions physically needed to keep global warming below 2°C. *Nature Communications*, *6*, 7958. https://doi.org/10.1038/ncomms8958

Giorgetta, M., Jungclaus, J., Reick, C., Legutke, S., Brovkin, V., Crueger, T., … Stevens, B. (2012). *CMIP5 Simulations of the Max Planck Institute for Meteorology (MPI-M) based on the MPI-ESM-LR model: The rcp45 Experiment, Served by ESGF*. World Data Center for Climate (WDCC) at DKRZ. https://doi.org/10.1594/WDCC/CMIP5.MXELr4

Giorgetta, M. A., Jungclaus, J., Reick, C. H., Legutke, S., Bader, J., Böttinger, M., … Stevens, B. (2013). Climate and carbon cycle changes from 1850 to 2100 in MPI-ESM simulations for the coupled model Intercomparison project phase 5. *Journal of Advances in Modeling Earth Systems*, *5*(3), 572–597. https://doi.org/10.1002/jame.20038

Giorgetta, M. A., Manzini, E., Roeckner, E., Esch, M., & Bengtsson, L. (2006). Climatology and forcing of the quasi-biennial oscillation in the MAECHAM5 model. *Journal of Climate*, *19*(16), 3882–3901. https://doi.org/10.1175/JCLI3830.1

Glienke, S., Irvine, P. J., & Lawrence, M. G. (2015). The impact of geoengineering on vegetation in experiment G1 of the GeoMIP. *Journal of Geophysical Research Atmospheres*, *120*(19), 10,196–10,213. https://doi.org/10.1002/2015JD024202

Hansen, J., Sato, M., Kharecha, P., von Schuckmann, K., Beerling, D. J., Cao, J., … Ruedy, R. (2017). Young people's burden: Requirement of negative CO_2 emissions. *Earth System Dynamics*, *8*(3), 577–616. https://doi.org/10.5194/esd-8-577-2017

Harding, A., & Moreno-Cruz, J. B. (2016). Solar geoengineering economics: From incredible to inevitable and half-way back. *Earth's Future*, *4*(12), 569–577. https://doi.org/10.1002/2016EF000462

Hartmann, J., West, A. J., Renforth, P., Köhler, P., De La Rocha, C. L., Wolf-Gladrow, D. A., … Scheffran, J. (2013). Enhanced chemical weathering as a geoengineering strategy to reduce atmospheric carbon dioxide, supply nutrients, and mitigate ocean acidification. *Reviews of Geophysics*, *51*(2), 113–149. https://doi.org/10.1002/rog.20004

Held, I. M., & Soden, B. J. (2006). Robust responses of the hydrological cycle to global warming. *Journal of Climate*, *19*(21), 5686–5699. https://doi.org/10.1175/jcli3990.1

Hong, Y., Moore, J. C., Jevrejeva, S., Ji, D., Phipps, S. J., Lenton, A., … Zhao, L. (2017). Impact of the GeoMIP G1 sunshade geoengineering experiment on the Atlantic meridional overturning circulation. *Environmental Research Letters*, *12*(3), 034,009. https://doi.org/10.1088/1748-9326/aa5fb8

Horton, J. B., Keith, D. W., & Honegger, M. (2016). Implications of the Paris agreement for carbon dioxide removal and solar geoengineering. In *Policy Brief, Harvard Project on Climate Agreements, Belfer Center for Science and International Affairs*. Cambridge, MA: Harvard Kennedy School.

House, J. I., Prentice, C. I., & Le Quéré, C. (2002). Maximum impacts of future reforestation or deforestation on atmospheric CO_2. *Global Change Biology*, *8*(11), 1047–1052. https://doi.org/10.1046/j.1365-2486.2002.00536.x

Hurtt, G., Chini, L., Frolking, S., Betts, R., Feddema, J., Fischer, G., … Wang, Y. (2011). Harmonization of land-use scenarios for the period 1500–2100: 600 years of global gridded annual land-use transitions, wood harvest, and resulting secondary lands. *Climatic Change*, *109*(1–2), 117–161. https://doi.org/10.1007/s10584-011-0153-2

Ilyina, T., Six, K. D., Segschneider, J., Maier-Reimer, E., Li, H., & Nunez-Riboni, I. (2013b). Global ocean biogeochemistry model HAMOCC: Model architecture and performance as component of the MPI-Earth system model in different CMIP5 experimental realizations. *Journal of Advances in Modeling Earth Systems*, *5*(2), 287–315. https://doi.org/10.1029/2012MS000178

Ilyina, T., Wolf-Gladrow, D., Munhoven, G., & Heinze, C. (2013a). Assessing the potential of calcium-based artificial ocean alkalinization to mitigate rising atmospheric CO_2 and ocean acidification. *Geophysical Research Letters*, *40*, 1–6. https://doi.org/10.1002/2013GL057981

Intergovernmental Panel on Climate Change (2012). *Meeting report of the intergovernmental panel on climate change expert meeting on geoengineering*. In O. Edenhofer, R. Pichs-Madruga, Y. Sokona, C. Field, V. Barros, T. F. Stocker, et al. (Eds.), *IPCC Working Group III Technical Support Unit* (p. 99). Potsdam, Germany: Potsdam Institute for Climate Impact Research.

Intergovernmental Panel on Climate Change (2013). Summary for policymakers. In T. F. Stocker, D. Qin, G.-K. Plattner, M. Tignor, S. K. Allen, J. Boschung, et al. (Eds.), *Climate Change 2013: The Physical Science Basis. Contribution of Working Group I to the Fifth Assessment Report of the Intergovernmental Panel on Climate Change*. Cambridge, England and New York, NY: Cambridge University Press.

Irvine, P. J., Kravitz, B., Lawrence, M. G., Gerten, D., Caminade, C., Gosling, S. N., … Smith, S. J. (2017). Towards a comprehensive climate impacts assessment of solar geoengineering. *Earth's Future*, *5*(1), 93–106. https://doi.org/10.1002/2016EF000389

Irvine, P. J., Kravitz, B., Lawrence, M. G., & Muri, H. (2016). An overview of the Earth system science of solar geoengineering. *WIREs Climate Change*, *7*, 815–833. https://doi.org/10.1002/wcc.423

Jones, C., Robertson, E., Arora, V., Friedlingstein, P., Shevliakova, E., Bopp, L., … Tjiputra, J. (2013). Twenty-first-century compatible CO_2 emissions and airborne fraction simulated by CMIP5 Earth system models under four representative concentration pathways. *Journal of Climate*, *26*(13), 4398–4413. https://doi.org/10.1175/jcli-d-12-00554.1

Jones, C. D., Ciais, P., Davis, S. J., Friedlingstein, P., Gasser, T., Peters, G. P., … Wiltshire, A. (2016). Simulating the Earth system response to negative emissions. *Environmental Research Letters*, *11*(9), 095,012. https://doi.org/10.1088/1748-9326/11/9/095012

Jungclaus, J. H., Fischer, N., Haak, H., Lohmann, K., Marotzke, J., Matei, D., … von Storch, J. S. (2013). Characteristics of the ocean simulations in the Max Planck Institute Ocean Model (MPIOM) the ocean component of the MPI-Earth system model. *Journal of Advances in Modeling Earth Systems*, *5*(2), 422–446. https://doi.org/10.1002/jame.20023

Keith, D. W., Wagner, G., & Zabel, C. L. (2017). Solar geoengineering reduces atmospheric carbon burden. *Nature Climate Change*, *7*(9), 617–619. https://doi.org/10.1038/nclimate3376

Keller, D. P., Feng, E. Y., & Oschlies, A. (2014). Potential climate engineering effectiveness and side effects during a high carbon dioxide-emission scenario. *Nature Communications*, *5*. https://doi.org/10.1038/ncomms4304

Keller, D. P., Lenton, A., Scott, V., Vaughan, N. E., Bauer, N., Ji, D., … Zickfeld, K. (2017). The carbon dioxide removal model Intercomparison project (CDR-MIP): Rationale and experimental design. *Geoscientific Model Development Discussions*, 1–72. https://doi.org/10.5194/gmd-2017-168

Kemena, T. P., Matthes, K., Martin, T., Wahl, S., & Oschlies, A. (2017). Atmospheric feedbacks in North Africa from an irrigated, afforested Sahara. *Climate Dynamics*. https://doi.org/10.1007/s00382-017-3890-8

Klepper, G., & Rickels, W. (2012). The real economics of climate engineering. *Economics Research International*, *2012*, 1–20. https://doi.org/10.1155/2012/316564

Klepper, G., & Rickels, W. (2014). Climate engineering: Economic considerations and research challenges. *Review of Environmental Economics and Policy*, *8*(2), 270–289. https://doi.org/10.1093/reep/reu010

Köhler, P., Abrams, J. F., Völker, C., Hauck, J., & Wolf-Gladrow, D. A. (2013). Geoengineering impact of open ocean dissolution of olivine on atmospheric CO_2, surface ocean pH and marine biology. *Environmental Research Letters*, *8*(1), 014,009. https://doi.org/10.1088/1748-9326/8/1/014009

Kracher, D. (2017). Nitrogen-related constraints of carbon uptake by large-scale forest expansion: Simulation study for climate change and management scenarios. *Earth's Future*, *5*(11), 1102–1118. https://doi.org/10.1002/2017EF000622

Kravitz, B., Caldeira, K., Boucher, O., Robock, A., Rasch, P. J., Alterskjær, K., … Yoon, J.-H. (2013a). Climate model response from the Geoengineering Model Intercomparison Project (GeoMIP). *Journal of Geophysical Research: Atmospheres*, *118*(15), 8320–8332. https://doi.org/10.1002/jgrd.50646

Kravitz, B., Robock, A., Forster, P. M., Haywood, J. M., Lawrence, M. G., & Schmidt, H. (2013b). An overview of the geoengineering model Intercomparison project (GeoMIP). *Journal of Geophysical Research: Atmospheres*, *118*(23), 13,103–13,107. https://doi.org/10.1002/2013JD020569

Kravitz, B., Robock, A., Tilmes, S., Boucher, O., English, J. M., Irvine, P. J., … Watanabe, S. (2015). The geoengineering model Intercomparison project phase 6 (GeoMIP6): Simulation design and preliminary results. *Geoscientific Model Development*, *8*(10), 3379–3392. https://doi.org/10.5194/gmd-8-3379-2015

Lawrence, D. M., Hurtt, A. A., Brovkin, V., Calvin, K. V., Jones, C. D., Lawrence, P. J., … Shevliakova, E. (2016). The Land Use Model Intercomparison Project (LUMIP): Rationale and experimental design. *Geoscientific Model Development*, *9*, 2973–2998. https://doi.org/10.5194/gmd-9-2973-2016

Matthews, H. D., & Caldeira, K. (2007). Transient climate–carbon simulations of planetary geoengineering. *Proceedings of the National Academy of Sciences of the United States of America*, *104*(24), 9949–9954. https://doi.org/10.1073/pnas.0700419104

Matthews, H. D., Cao, L., & Caldeira, K. (2009). Sensitivity of ocean acidification to geoengineered climate stabilization. *Geophysical Research Letters*, *36*(10), L10,706. https://doi.org/10.1029/2009GL037488

McCormack, C. G., Born, W., Irvine, P. J., Achterberg, E. P., Amano, T., Ardron, J., … Sutherland, W. J. (2016). Key impacts of climate engineering on biodiversity and ecosystems, with priorities for future research. *Journal of Integrative Environmental Sciences*, 1–26. https://doi.org/10.1080/1943815X.2016.1159578

Moriyama, R., Sugiyama, M., Kurosawa, A., Masuda, K., Tsuzuki, K., & Ishimoto, Y. (2017). The cost of stratospheric climate engineering revisited. *Mitigation and Adaptation Strategies for Global Change*, *22*(8), 1207–1228. https://doi.org/10.1007/s11027-016-9723-y

National Research Council (2015a). *Climate Intervention: Carbon Dioxide Removal and Reliable Sequestration*. Washington, DC: The National Academies Press. https://doi.org/10.17226/18805

National Research Council (2015b). *Climate Intervention: Reflecting Sunlight to Cool Earth*. Washington, DC: The National Academies Press. https://doi.org/10.17226/18988

Niemeier, U., Schmidt, H., Alterskjær, K., & Kristjánsson, J. E. (2013). Solar irradiance reduction via climate engineering: Impact of different techniques on the energy balance and the hydrological cycle. *Journal of Geophysical Research: Atmospheres*, *118*(21), 11,905–11,917. https://doi.org/10.1002/2013JD020445

Niemeier, U., & Tilmes, S. (2017). Sulfur injections for a cooler planet. *Science*, *357*(6348), 246–248. https://doi.org/10.1126/science.aan3317

Niemeier, U., & Timmreck, C. (2015). What is the limit of climate engineering by stratospheric injection of SO_2? *Atmospheric Chemistry and Physics*, *15*(16), 9129–9141. https://doi.org/10.5194/acp-15-9129-2015

Ornstein, L., Aleinov, I., & Rind, D. (2009). Irrigated afforestation of the Sahara and Australian outback to end global warming. *Climatic Change*, *97*(3–4), 409–437. https://doi.org/10.1007/s10584-009-9626-y

Oschlies, A., Held, H., Keller, D., Keller, K., Mengis, N., Quaas, M., … Schmidt, H. (2016). Indicators and metrics for the assessment of climate engineering. *Earth's Future*, *5*(1), 49–58. https://doi.org/10.1002/2016EF000449

Oschlies, A., & Klepper, G. (2017). Research for assessment, not deployment, of climate engineering: The German Research Foundation's priority program SPP 1689. *Earth's Future*, *5*(1), 128–134. https://doi.org/10.1002/2016EF000446

Parson, E. A. (2017). Opinion: Climate policymakers and assessments must get serious about climate engineering. *Proceedings of the National Academy of Sciences of the United States of America*, *114*(35), 9227–9230. https://doi.org/10.1073/pnas.1713456114

Pitari, G., Aquila, V., Kravitz, B., Robock, A., Watanabe, S., Cionni, I., … Tilmes, S. (2014). Stratospheric ozone response to sulfate geoengineering: Results from the geoengineering model Intercomparison project (GeoMIP). *Journal of Geophysical Research*, *119*(5), 2629–2653. https://doi.org/10.1002/2013JD020566

Pongratz, J., Lobell, D. B., Cao, L., & Caldeira, K. (2012). Crop yields in a geoengineered climate. *Nature Climate Change*, *2*(2), 101–105. https://doi.org/10.1038/nclimate1373

Pongratz, J., Reick, C. H., Raddatz, T., Caldeira, K., & Claussen, M. (2011). Past land use decisions have increased mitigation potential of reforestation. *Geophysical Research Letters*, *38*(15), L15,701. https://doi.org/10.1029/2011GL047848

Reick, C., Giorgetta, M., Jungclaus, J., Legutke, S., Brovkin, V., Crueger, T., … Stevens, B. (2012a). *CMIP5 Simulations of the Max Planck Institute for Meteorology (MPI-M) based on the MPI-ESM-LR Model: The esmrcp85 experiment, Served by ESGF*. World Data Center for Climate (WDCC) at DKRZ. https://doi.org/10.1594/WDCC/CMIP5.MXELe8

Reick, C., Giorgetta, M., Jungclaus, J., Legutke, S., Brovkin, V., Crueger, T., … Stevens, B. (2012b). *CMIP5 Simulations of the Max Planck Institute for Meteorology (MPI-M) based on the MPI-ESM-LR Model: The esmHistorical Experiment, Served by ESGF*. World Data Center for Climate (WDCC) at DKRZ. https://doi.org/10.1594/WDCC/CMIP5.MXELeh

Reick, C. H., Raddatz, T., Brovkin, V., & Gayler, V. (2013). Representation of natural and anthropogenic land cover change in MPI-ESM. *Journal of Advances in Modeling Earth Systems*, *5*(3), 459–482. https://doi.org/10.1002/jame.20022

Renforth, P., & Henderson, G. (2017). Assessing ocean alkalinity for carbon sequestration. *Reviews of Geophysics*, *55*, 636–674. https://doi.org/10.1002/2016RG000533

Riahi, K., Rao, S., Krey, V., Cho, C., Chirkov, V., Fischer, G., … Rafaj, P. (2011). RCP 8.5—A scenario of comparatively high greenhouse gas emissions. *Climatic Change*, *109*(1–2), 33–57. https://doi.org/10.1007/s10584-011-0149-y

Rickels, W., Klepper, G., Dovern, J., Betz, G., Brachatzek, N., Cacean, S., … Zürn, M. (2011). *Large-Scale Intentional Interventions into the Climate System? Assessing the Climate Engineering Debate. Scoping report conducted on behalf of the German Federal Ministry of Education and Research (BMBF)* (Tech. Rep.). Kiel: Kiel Earth Institute.

Robock, A., Oman, L., & Stenchikov, G. L. (2008). Regional climate responses to geoengineering with tropical and Arctic SO_2 injections. *Journal of Geophysical Research: Atmospheres*, *113*, D16,101. https://doi.org/10.1029/2008JD010050

Royal Society (2009). *Geoengineering the Climate: Science, Governance and Uncertainty* (RS policy document 10/09). London, England: The Royal Society.

Russell, L. M., Rasch, P. J., Mace, G. M., Jackson, R. B., Shepherd, J., Liss, P., … Morgan, M. G. (2012). Ecosystem impacts of geoengineering: A review for developing a science plan. *Ambio*, *41*(4), 350–369. https://doi.org/10.1007/s13280-012-0258-5

Sanderson, B. M., O'Neill, B. C., & Tebaldi, C. (2016). What would it take to achieve the Paris temperature targets? *Geophysical Research Letters*, *43*(13), 7133–7142. https://doi.org/10.1002/2016GL069563

Schaefer, K., Lantuit, H., Romanovsky, V. E., Schuur, E. A. G., & Witt, R. (2014). The impact of the permafrost carbon feedback on global climate. *Environmental Research Letters*, *9*(8), 085,003. https://doi.org/10.1088/1748-9326/9/8/085003

Schäfer, S., Lawrence, M., Stelzer, H., Born, W., Low, S., Aaheim, A., … Vaughan, N. (2015). The European Transdisciplinary Assessment of Climate Engineering (EuTRACE): Removing Greenhouse Gases from the Atmosphere and Reflecting Sunlight away from Earth, Funded by the European Union's Seventh Framework Programme under Grant Agreement 306993.

Schmidt, H., Alterskjær, K., Bou Karam, D., Boucher, O., Jones, A., Kristjánsson, J. E., … Timmreck, C. (2012). Solar irradiance reduction to counteract radiative forcing from a quadrupling of CO_2: Climate responses simulated by four Earth system models. *Earth System Dynamics*, *3*(1), 63–78. https://doi.org/10.5194/esd-3-63-2012

Seneviratne, S. I., Donat, M. G., Pitman, A. J., Knutti, R., & Wilby, R. L. (2016). Allowable CO_2 emissions based on regional and impact-related climate targets. *Nature*, *529*(7587), 477–483. https://doi.org/10.1038/nature16542

Sitch, S., Brovkin, V., von Bloh, W., van Vuuren, D., Eickhout, B., & Ganopolski, A. (2005). Impacts of future land cover changes on atmospheric CO_2 and climate. *Global Biogeochemical Cycles*, *19*(2), GB2013. https://doi.org/10.1029/2004GB002311

Sonntag, S., Pongratz, J., Reick, C. H., & Schmidt, H. (2016). Reforestation in a high-CO_2 world—Higher mitigation potential than expected, lower adaptation potential than hoped for. *Geophysical Research Letters*, *43*(12), 6546–6553. https://doi.org/10.1002/2016GL068824

Stevens, B., Giorgetta, M., Esch, M., Mauritsen, T., Crueger, T., Rast, S., … Roeckner, E. (2013). Atmospheric component of the MPI-M Earth system model: ECHAM6. *Journal of Advances in Modeling Earth Systems*, *5*(2), 146–172. https://doi.org/10.1002/jame.20015

Stier, P., Feichter, J., Kinne, S., Kloster, S., Vignati, E., Wilson, J., … Petzold, A. (2005). The aerosol-climate model ECHAM5-HAM. *Atmospheric Chemistry and Physics*, *5*(4), 1125–1156. https://doi.org/10.5194/acp-5-1125-2005

Thomson, A. M., Calvin, K. V., Smith, S. J., Kyle, G. P., Volke, A., Patel, P., … Edmonds, J. A. (2011). RCP4.5: A pathway for stabilization of radiative forcing by 2100. *Climatic Change*, *109*(1–2), 77–94. https://doi.org/10.1007/s10584-011-0151-4

Tilmes, S., Fasullo, J., Lamarque, J.-F., Marsh, D. R., Mills, M., Alterskjaer, K., … Watanabe, S. (2013). The hydrological impact of geoengineering in the geoengineering model Intercomparison project (GeoMIP). *Journal of Geophysical Research: Atmospheres*, *118*(19), 11,036–11,058. https://doi.org/10.1002/jgrd.50868

Tjiputra, J. F., Grini, A., & Lee, H. (2016). Impact of idealized future stratospheric aerosol injection on the large-scale ocean and land carbon cycles. *Journal of Geophysical Research: Biogeosciences*, *121*(1). https://doi.org/10.1002/2015JG003045

Trenberth, K. E., & Dai, A. (2007). Effects of Mount Pinatubo volcanic eruption on the hydrological cycle as an analog of geoengineering. *Geophysical Research Letters*, *34*(15), L15,702. https://doi.org/10.1029/2007GL030524

United Nations Framework Convention on Climate Change (2012). *Report of the Conference of the Parties serving as the meeting of the Parties to the Kyoto Protocol on its seventh session, held in Durban from 28 November to 11 December 2011. Addendum. Part two: Action taken by the Conference of the Parties serving as the meeting of the Parties to the Kyoto Protocol at its seventh session* (Tech. Rep.). Geneva, Switzerland: United Nations Office.

United Nations Framework Convention on Climate Change (2015). Adoption of the Paris Agreement. In *21st Conference of the Parties*. Paris: United Nations.

Vaughan, N. E., & Lenton, T. M. (2011). A review of climate geoengineering proposals. *Climatic Change*, *109*(3–4), 745–790. https://doi.org/10.1007/s10584-011-0027-7

Victor, D. G. (2008). On the regulation of geoengineering. *Oxford Review of Economic Policy*, *24*(2), 322–336. https://doi.org/10.1093/oxrep/grn018

Williamson, P. (2016). Emissions reduction: Scrutinize CO_2 removal methods. *Nature*, *530*, 153–155. https://doi.org/10.1038/530153a

Xia, L., Robock, A., Tilmes, S., & Neely III, R. R. (2016). Stratospheric sulfate geoengineering could enhance the terrestrial photosynthesis rate. *Atmospheric Chemistry and Physics*, *16*(3), 1479–1489. https://doi.org/10.5194/acp-16-1479-2016

Zickfeld, K., Eby, M., Weaver, A. J., Alexander, K., Crespin, E., Edwards, N. R., … Zhao, F. (2013). Long-term climate change commitment and reversibility: An EMIC Intercomparison. *Journal of Climate*, *26*(16), 5782–5809. https://doi.org/10.1175/JCLI-D-12-00584.1

Zwiers, F. W., & von Storch, H. (1995). Taking serial correlation into account in tests of the mean. *Journal of Climate*, *8*(2), 336–351. https://doi.org/10.1175/1520-0442(1995)008<0336:tsciai>2.0.co;2